

**ANALYSIS OF A TIMBER-CONCRETE UNIT  
SUPPORTED BY A STEEL FRAME**



Bachelor's thesis  
Construction Engineering  
Spring 2021  
Joseph James

BEng (Poly), Build. Construct.

Degree Programme in Construction Engineering

Author Joseph James

Subject Analysis of a timber-concrete unit supported by a steel frame

Supervisors Cristina Tirteau

Abstract

Year 2021

---

The purpose of this thesis is to carry out an analysis of a timber-concrete unit supported by a steel frame. This analysis will be conducted on a five-story apartment building being designed and engineered by WAY Structural Technology in Vantaa, Finland. The main goal is to find the interaction between the different materials to determine the required contact points between the units and the frame. To accomplish this, first the structure was analysed to find critical points for further analysis and preliminary calculations were conducted by hand to determine internal forces, deflections and capacities of key load bearing elements. Next, the structure was modelled in different ways to find the most appropriate and applicable solution. Finally, the modelling solution found in the previous step was simplified and used to analyse the deflections and determine the required contact points.

Keywords Structural analysis, Structural engineering, Structural modeling

Pages 62 pages

# Contents

1	Introduction .....	1
1.1	General background.....	1
1.2	Objectives.....	1
1.3	Knowledge Base.....	2
1.4	Framework and Tools.....	2
2	The Structure .....	3
2.1	The Building Structure.....	3
2.2	The Timber-Concrete Unit Structure .....	4
3	Manual Analysis.....	5
3.1	Manual Analysis of Loads .....	6
3.2	Manual Analysis of the Steel Beams.....	8
3.2.1	Results.....	12
3.3	Manual Analysis of the LVL.....	12
3.3.1	Results.....	19
4	Analysis Using Structural Design Software (RFEM) .....	19
5	Simplified Models to Verify Manual LVL Calculations .....	19
5.1	Results .....	23
6	Detailed Models to Analyse the Behaviour of the Structure .....	23
6.1	Detailed Model with LVL as a Member.....	24
6.1.1	Results.....	29
6.2	Detailed Model with LVL as a Surface.....	30
6.2.1	Results.....	34
6.3	Analysis of Hinge Configurations in Detailed Surface Model.....	34
6.3.1	Results.....	38
7	Simplified Analysis to Determine Size and Locations of the Sylomer Pads .....	39
7.1	Single Solid Wall, CFRHS200x200x12.5 beam .....	39
7.1.1	Results.....	43
7.2	Double Solid Wall, CFRHS200x200x12.5 beam .....	46
7.2.1	Results.....	47
7.3	Single wall with opening, CFRHS200x200x12.5 beam .....	49

7.3.1 Results.....	52
7.4 Double wall with opening, CFRHS200x200x12.5 beam .....	54
7.4.1 Results.....	57
8 Conclusion .....	58
References .....	62

# 1 Introduction

## 1.1 General background

In the construction industry, there is a continual need for developing new structural systems that allow for fast on-site construction by taking advantage of industrial production. At the same time, environmental concerns have created a high demand for high-rise structures which utilize sustainable materials such as timber. While research in fire design and development of pre-engineered timber such as glulam, laminated veneer lumber (LVL) and cross-laminated timber (CLT) have increased the possibilities of using timber in larger buildings, its use is limited by its weaker material properties. One solution to these circumstances is to develop a modular building system that is fast and easy to install and features timber as the primary material in the living space and steel as the building frame.

The incorporation of steel, concrete and timber in a single structure presents challenging design problems. Due to the lack of design standards and handbooks for designing structures composed of multiple materials, creative thinking and innovative use of engineering methods must be utilized. Structural engineering experience and expertise is an essential aspect of this process, allowing the designer to see the bigger picture and approach the design in unconventional ways. The complexity of the whole building must be simplified into individual design scenarios where solutions are found and incorporated back into the overall structure.

## 1.2 Objectives

The purpose of this thesis is to carry out an analysis of a timber-concrete unit supported by a steel frame. This analysis will be conducted on a five-story apartment building being designed and engineered by WAY Structural Technology in Vantaa, Finland. The main goal is to find the interaction between the different materials to determine the required contact points between the units and the frame. To accomplish this, an appropriate way of modelling the situation must first be found. Then, deflections can be analysed to determine the placement of composite connections and contact points between the units and the frame.

The solutions found in this thesis work will be used to develop the building system as a new product.

### **1.3 Knowledge Base**

There is no knowledge base for this type of building system. While there are companies who have developed timber-based modular building systems, for example Stora Enso, it is a new method and is not currently in widespread use. In addition, steel framing and composite concrete floors are not typically utilized in the design of modular systems involving the use of wood.

### **1.4 Framework and Tools**

This is a practice-based thesis which deals with the following key research questions.

- What material primarily carries the loads from the units?
- What is the best way to model the design situation?
- How do the timber-concrete units interact with the steel frame?
- What contact points are needed between the frame and units?

To find the answers to these questions, first the building was analysed to find a critical zone, i.e. an area in the structure where the loads and geometry lead to the largest forces. To simplify the calculations, this critical zone was then isolated from the rest of the structure for further analysis. Preliminary calculations were then conducted by hand to determine internal forces, deflections and capacities of key load bearing elements. Next, the structure was modelled in different ways to find the most appropriate and applicable solution. Finally, the modelling solution found in the previous step was simplified and used to analyse the deflections and determine the required contact points. The structural design software used in carrying out this process were Trimble Tekla Structures and Dlubal RFEM. In addition, Eurocode structural design standards and company expertise and advice were utilized. The starting point of this thesis was a preliminary 3d model in Tekla Structures.

## 2 The Structure

### 2.1 The Building Structure

The overall structure of the building consists of a steel frame which carries loads from interior concrete-timber units and exterior thermal-element façade structures. A global bracing system is not utilized in the structure. The concrete stairwell in the centre of the building is used for horizontal stability. Since the purpose of this thesis is to determine the interaction between the concrete-timber units and the steel frame, horizontal forces and the exterior facade structures have not been considered.

Figure 1. Initial Tekla model of the structure with facades visible.

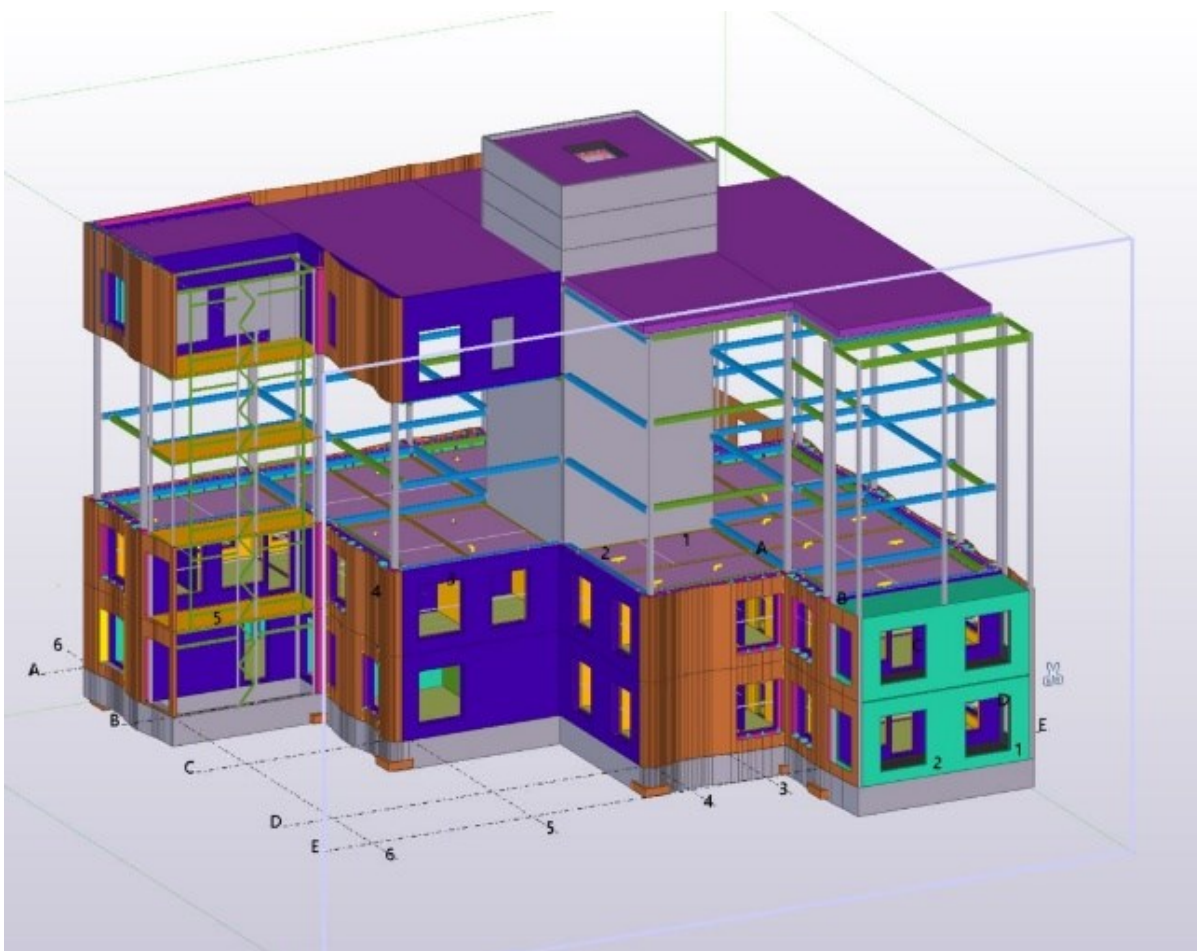
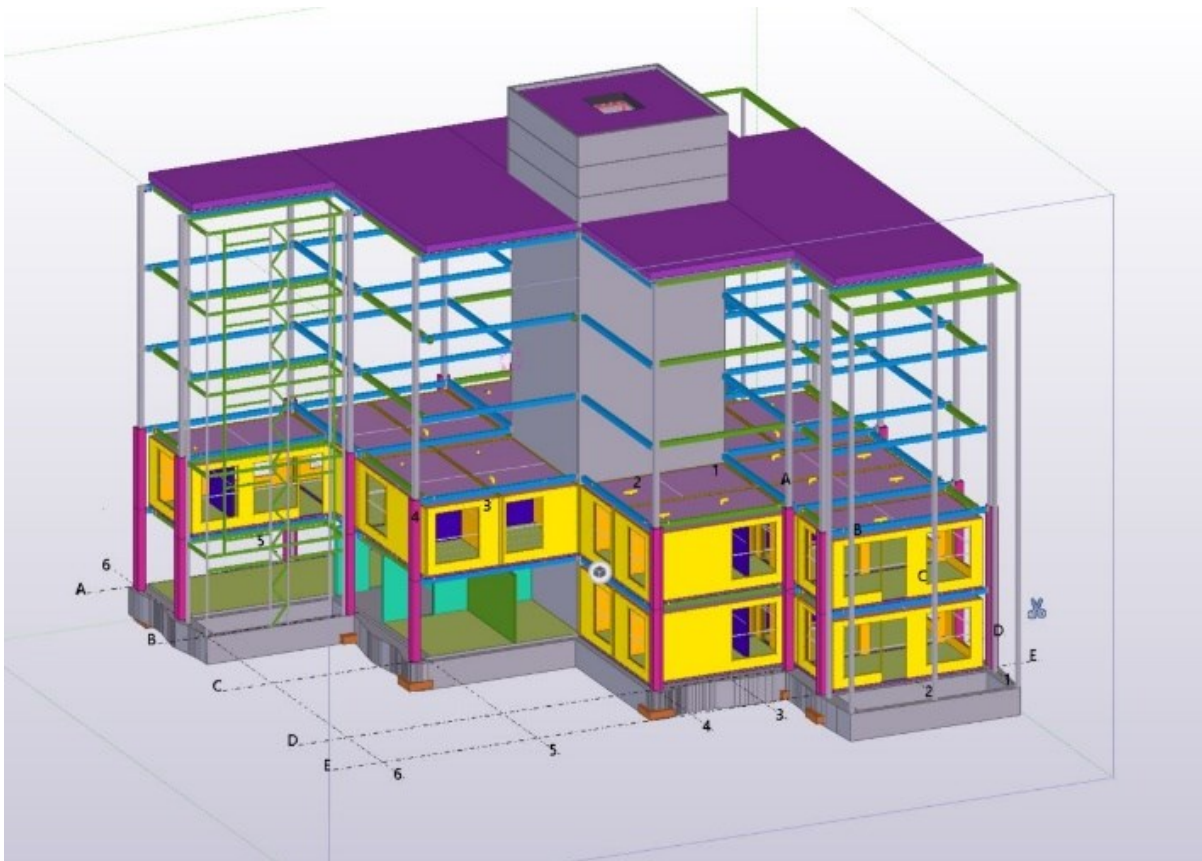


Figure 2. Initial Tekla model of the structure with facades hidden.

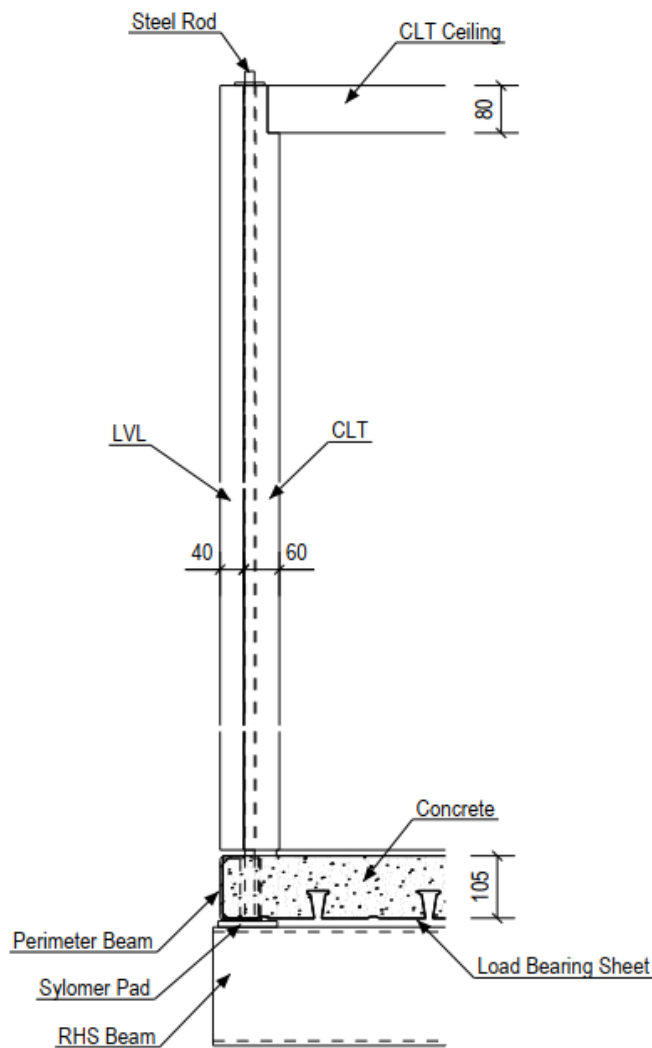


## 2.2 The Timber-Concrete Unit Structure

The structure of the timber-concrete units consists of LVL-CLT composite walls and one-way load bearing concrete-steel sheet floor structures. The LVL is designed to be the load bearing element of the wall structure to which the CLT is attached with screws and the floor structure is attached via steel rods. The units sit on the steel frame of the building, resting on sylomer pads.



Figure 3. Section view of the timber-concrete unit, steel beam and sylomer pad.



### 3 Manual Analysis

The purpose of first conducting a manual analysis was to gain an initial understanding of the structure and to have an idea of values to be expected in further calculations. Loads were analyzed to find values for self-weight and to identify a critical zone. A preliminary investigation of the steel beams was then carried out to check beam profiles for strength. Lastly, an analysis was made of the LVL beam to verify the strength of a full wall and determine the minimum height of a full span opening.

### 3.1 Manual Analysis of Loads

Analysis began with an overall assessment of the structure. Consideration was given to the different design situations and configurations that occur in the building so that the most critical area could be identified for further analysis. Given the identical geometry of each floor plan, the second story was selected as the focus. Each module on the selected story was analysed to determine which module produces the largest load. The self-weight was calculated by considering the area of the materials without openings.

Figure 4. Calculation of the self weight of the timber-concrete unit.

**Beam forces and deflections using heaviest module unit weight per square meter as uniform distributed load over entire building (wall openings not taken into account):**

Self weight of Module

Concrete -	$g_{conc} := 25 \frac{kN}{m^3} \cdot 0.1 m$	$g_{conc} = 2.5 \frac{kN}{m^2}$
Composite sheet -	$g_{cs} := 11.78 \frac{kg}{m^2} \cdot 10 \frac{m}{s^2}$	$g_{cs} = 0.118 \frac{kN}{m^2}$
CLT Ceiling -	$g_{CLTc} := 5 \frac{kN}{m^3} \cdot 0.08 m$	$g_{CLTc} = 0.4 \frac{kN}{m^2}$
CLT, ext. walls -	$g_{CLTew} := 5 \frac{kN}{m^3} \cdot \frac{(0.06 m \cdot 2.67 m \cdot 18.64 m)}{19.4 m^2}$	$g_{CLTew} = 0.77 \frac{kN}{m^2}$
CLT, int. walls -	$g_{CLTiw} := 5 \frac{kN}{m^3} \cdot \frac{(0.1 m \cdot 2.59 m \cdot 6.2 m)}{19.4 m^2}$	$g_{CLTiw} = 0.414 \frac{kN}{m^2}$
LVL, ext. walls -	$g_{LVLe} := 5.1 \frac{kN}{m^3} \cdot \frac{(0.04 m \cdot 2.67 m \cdot 18.64 m)}{19.4 m^2}$	$g_{LVLe} = 0.523 \frac{kN}{m^2}$
Perimeter beam -	$g_{pb} := 0.065 \frac{kN}{m} \cdot \frac{(18.64 m)}{19.4 m^2}$	$g_{pb} = 0.062 \frac{kN}{m^2}$
	$g_k := g_{conc} + g_{cs} + g_{CLTc} + g_{CLTew} + g_{CLTiw} + g_{LVLe} + g_{pb}$	$g_k = 4.787 \frac{kN}{m^2}$

From these calculations, it was determined that a critical loading occurs around modules 1, 3 and 5, and therefore this section of the building would be focused on for further analysis.

Figure 5. Layout of the building with the critical zone.

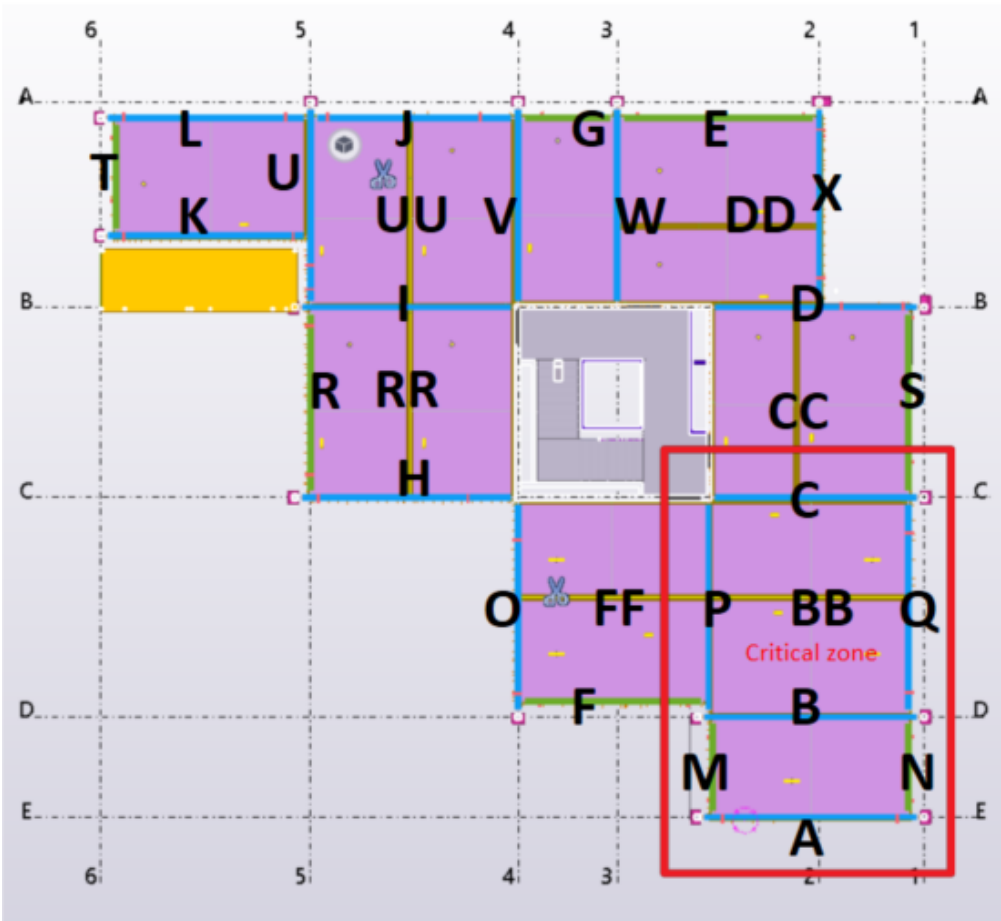
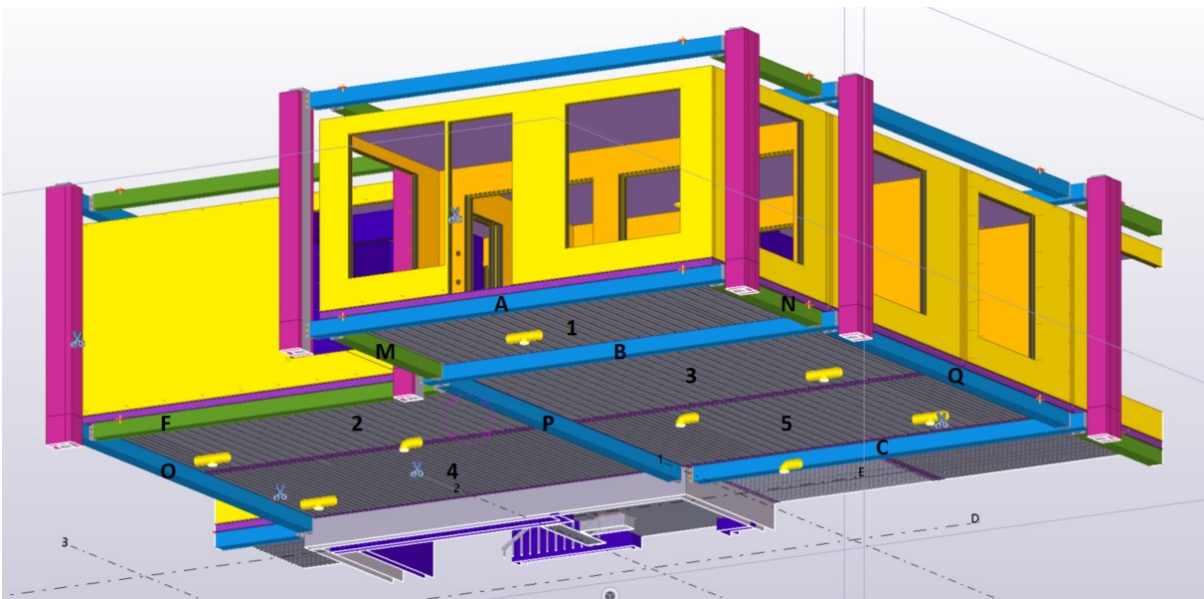


Figure 6. Three dimensional view of the critical zone.



### **3.2 Manual Analysis of the Steel Beams**

The dead and live load from the timber-concrete units were then applied directly to the steel frame to determine preliminary internal forces and deflections of the steel beams in this area of the building. From these calculations, the beam cross-section of beam B (see Fig. 5, 6, and 7) was found to be deflecting beyond requirements set out in the Finnish National Annex to Eurocode SFS-EN 1993-1-1 for the serviceability limit state (SLS) (Finnish Ministry of the Environment, 2019, p.19). After taking the dead load into account with pre-cambering, some additional calculations were then made using alternative beam cross-sections (see Fig. 8 and 9).

Figure 7. Manual analysis of a CFRHS200x200x8 beam.

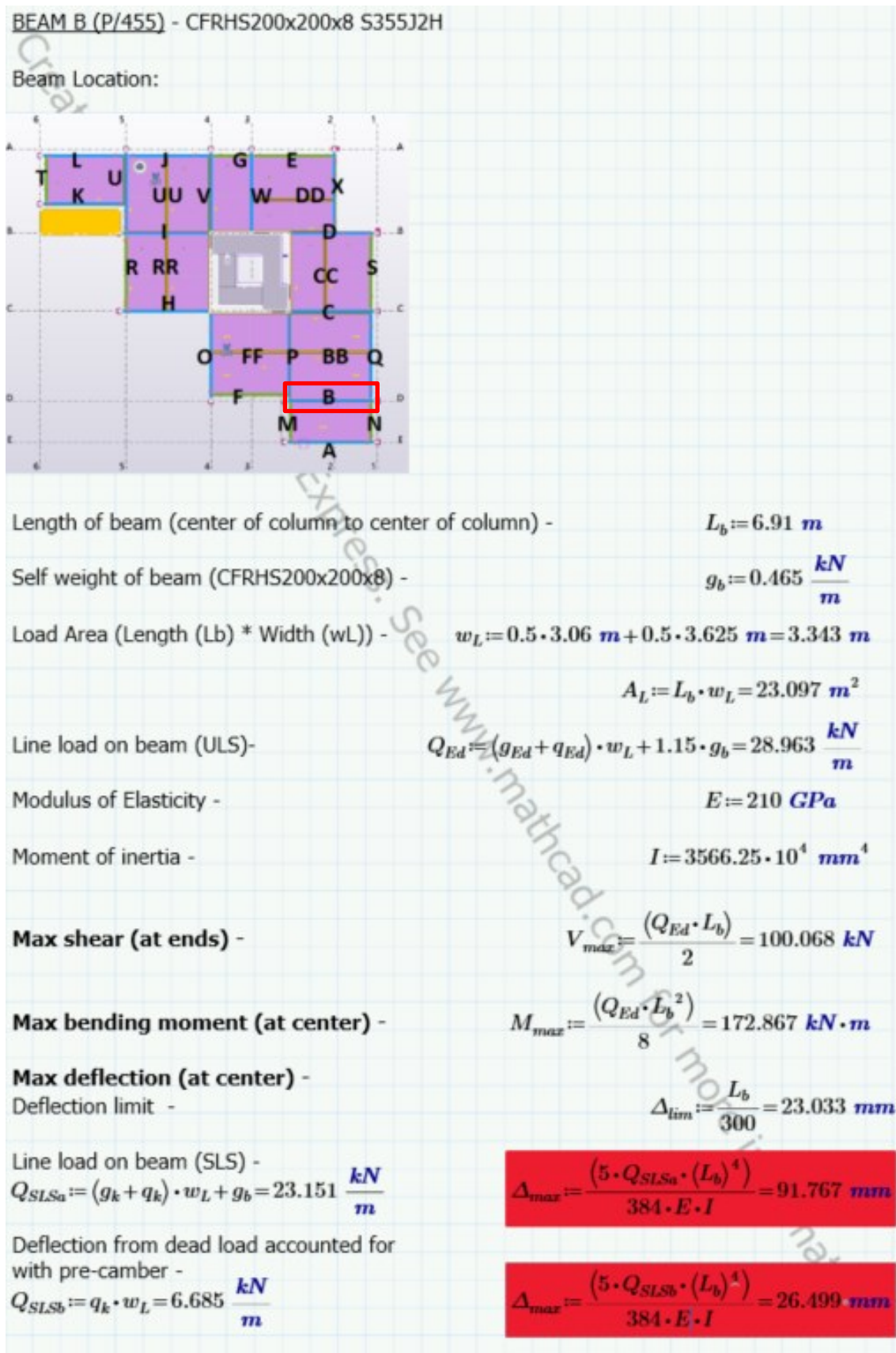


Figure 8. Manual analysis of a CFRHS200x200x12.5 beam.

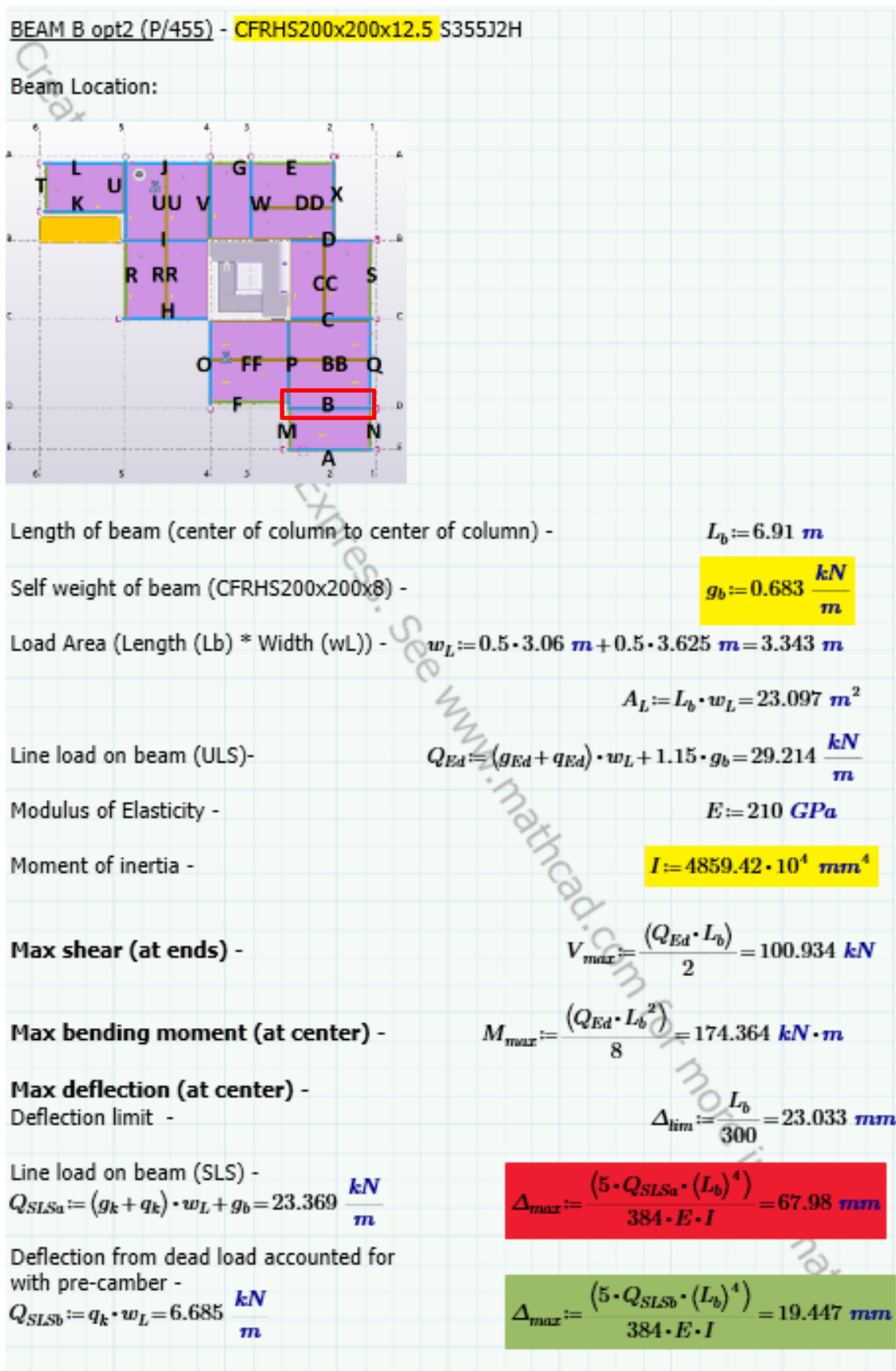
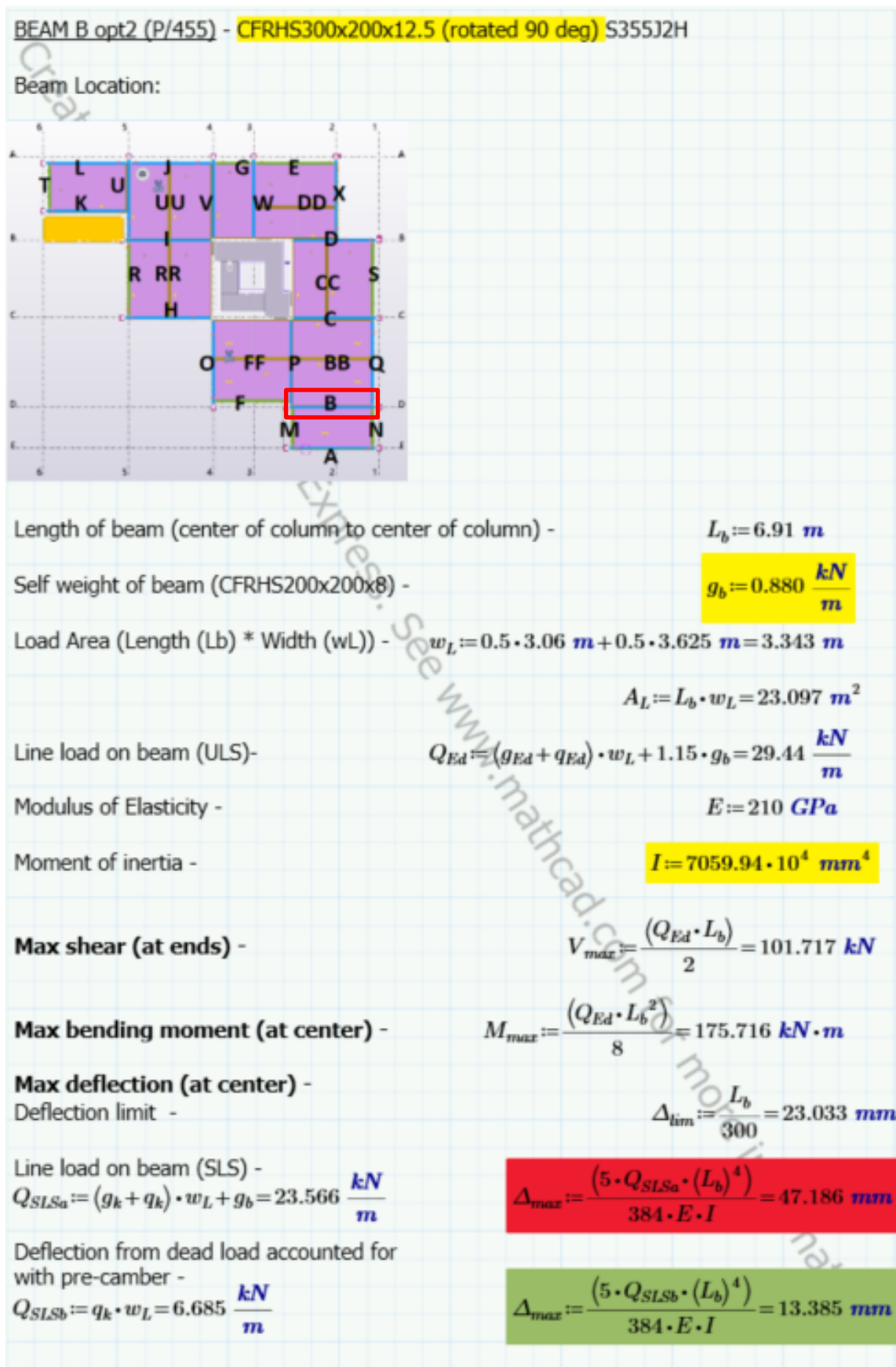


Figure 9. Manual analysis of a CFRHS300x200x12.5 beam rotated 90 degrees.



### 3.2.1 Results

Initial SLS analysis of the steel beams showed that the thickness of the profile would need to be increased to 12.5 mm and that pre-cambering would be necessary in all the beam profiles analyzed above. Further ultimate limit state (ULS) analysis of the beams and connection details will be required.

### 3.3 Manual Analysis of the LVL

Next, the critical location identified above was used to analyse the load bearing capacity of the LVL. The idea was to find out what LVL wall dimensions would support the dead load of the CLT and concrete. The 40mm thick LVL wall was treated as a beam, carrying the dead loads of the CLT and concrete, and the live load from the concrete floor surface. The loads were applied to a full LVL wall without window or door openings, 40mm thick and 2725 mm high. The maximum bending moment of the solid LVL wall was found, then the resistance of the LVL beam was calculated according to Eurocode SFS-EN 1995-1-1 using Puurakenteiden lyhennetty suunnitteluohje (PUUINFO, 2020, p. 15-18). The capacity of the solid wall was verified and the minimum height of the LVL, was determined (see Fig. 10 - 15).

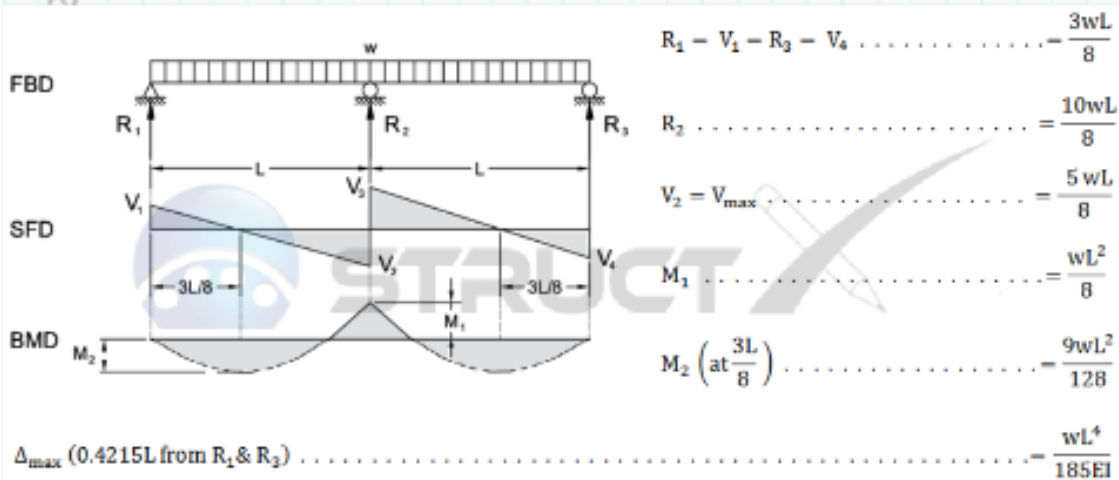


Figure 10. LVL analysis, page 1.

<b>LVL BEAM - Analysis</b>		
<u>Self weight</u>		
Concrete -	$g_{conc} := 25 \frac{kN}{m^3} \cdot 0.1 m \cdot \frac{3.05 m}{2}$	$g_{conc} = 3.813 \frac{kN}{m}$
Composite sheet -	$g_{cs} = 11.78 \frac{kg}{m^2} \cdot 10 \frac{m}{s^2} \cdot \frac{3.05 m}{2}$	$g_{cs} = 0.18 \frac{kN}{m}$
Perimeter beam -	$g_{pb} = 0.065 \frac{kN}{m}$	$g_{pb} = 0.065 \frac{kN}{m}$
CLT Ceiling -	$g_{CLTc} := 5 \frac{kN}{m^3} \cdot 0.08 m \cdot \frac{3.05 m}{2}$	$g_{CLTc} = 0.61 \frac{kN}{m}$
CLT, ext. walls -	$g_{CLTew} := 0.77 \frac{kN}{m^2} \cdot \frac{3.05 m}{2}$	$g_{CLTew} = 1.174 \frac{kN}{m}$
CLT, int. walls -	$g_{CLTiw} := 0.414 \frac{kN}{m^2} \cdot \frac{3.05 m}{2}$	$g_{CLTiw} = 0.631 \frac{kN}{m}$
LVL, ext. walls -	$g_{LVLew} := 0.523 \frac{kN}{m^2} \cdot \frac{3.05 m}{2}$	$g_{LVLew} = 0.798 \frac{kN}{m}$
	$g_k := g_{conc} + g_{cs} + g_{CLTc} + g_{CLTew} + g_{CLTiw} + g_{LVLew} + g_{pb}$	$g_k = 7.27 \frac{kN}{m}$
<u>Live load</u>		
	$q_k := 2.0 \frac{kN}{m^2} \cdot \frac{3.05 m}{2}$	$q_k = 3.05 \frac{kN}{m}$
<u>Characteristic load</u>		
	$w_k := g_k + q_k$	$w_k = 10.32 \frac{kN}{m}$
<u>Critical load combination for beams</u>		
1.15 * Dead load + 1.5 * Live load		
<u>Design load</u>		
	$w_{Ed} := 1.15 \cdot g_k + 1.5 \cdot q_k$	$w_{Ed} = 12.936 \frac{kN}{m}$

Figure 11. LVL analysis, page 2.

Force from concrete on the beam, calculated as a point load at  $L=3085\text{mm}$  (half of beam span):



Structx. (2021). Beam Design Formulas: Continuous Beams – Two Equal Spans with UDL. Retrieved from [https://structx.com/Beam\\_Formulas\\_041.html](https://structx.com/Beam_Formulas_041.html)

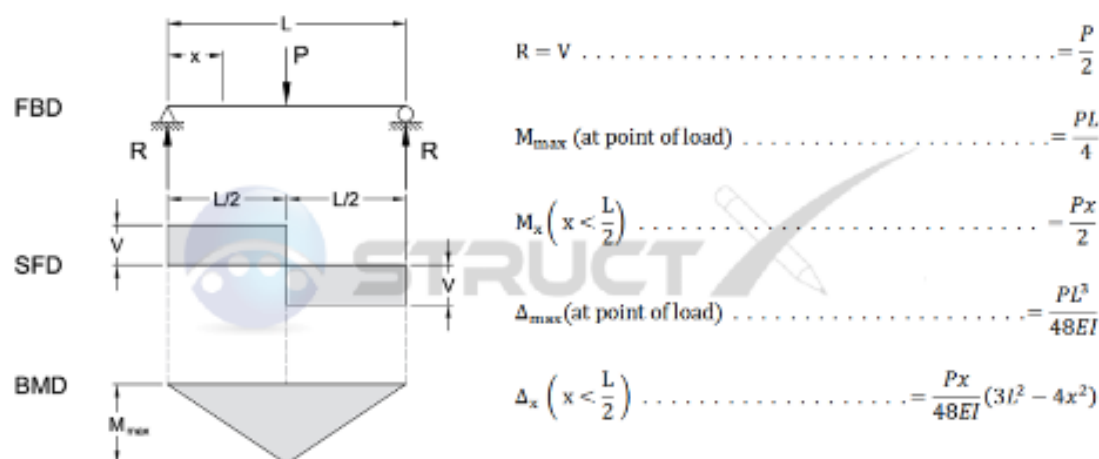
Calculation of the reaction force (R2)

$L = 3.085 \text{ m}$

$$R_{2ULS} = \frac{(10 \cdot w_{Ed} \cdot L)}{8} \qquad R_{2ULS} = 49.884 \text{ kN}$$

$$R_{2SLS} = \frac{(10 \cdot w_k \cdot L)}{8} \qquad R_{2SLS} = 39.798 \text{ kN}$$

Calculation of the max moment from force of the concrete floor as a point load  $L=6170\text{mm}$  (whole beam span) using the following table:



Structx. (2021). Beam Design Formulas: Simple Beam – Point load at center. Retrieved from [https://structx.com/Beam\\_Formulas\\_007.html](https://structx.com/Beam_Formulas_007.html)

Figure 12. LVL analysis, page 3.

$$L := 6.17 \text{ m} \quad b_{LVL} := 40 \text{ mm} \quad h_{LVL} := 2725 \text{ mm}$$

$$M_{max} := \frac{(R_{2ULS} \cdot L)}{4} = 76.946 \text{ kN} \cdot \text{m}$$

Resistance of LVL beam

$$b_{LVL} := 40 \text{ mm} \quad h_{LVL} := 2725 \text{ mm}$$

$$E = 10500 \frac{\text{N}}{\text{mm}^2} \quad J := \frac{(b_{LVL} \cdot h_{LVL}^3)}{12}$$

$$W := \frac{(b_{LVL} \cdot h_{LVL}^2)}{6} = (4.95 \cdot 10^7) \text{ mm}^3$$

$$\sigma_m := \frac{M_{max}}{W} = 1.554 \text{ MPa}$$

Created with PTC Mathcad Express. See [www.mathcad.com](http://www.mathcad.com) for more information.

Figure 13. LVL analysis, page 4.

Kun syrjällään taivutetun LVL-palkin korkeus on yli 300 mm, taivutuslujuuden ominaisarvoa  $f_{m,k}$  pienennetään kertoimella  $k_h$ :

$$k_h = \left( \frac{300}{h} \right)^2 \leq 1,2 \quad (3.1)$$

missä

$h$  palkin korkeus [mm]

$s$  kokovaikutuseksponentti (ks. taulukko 3.4)

(PUUINFO, 2020, p. 16)

Tyyppi		Kerto-S	Kerto-T	Kerto-Q
Paksuus (mm)		21 - 90	27 - 75	27 - 69
<b>Ominaislujuudet (N/mm<sup>2</sup>)</b>				
Taivutus syrjällään	$f_{m,k}$	44	27	32
Kokovaikutuseksponentti	$s$	0,12	0,15	0,12
Taivutus lappeellaan	$f_{m,0,MLA}$	50	32	36
Veto syysuuntaan	$f_{t,k}$	35	24	26
Veto poikittain syrjällään	$f_{t,90,MLA}$	0,8	0,5	6,0
Puristus syysuuntaan	$f_{c,k}$	35	26	26
Puristus poikittain syrjällään	$f_{c,90,MLA}$	6	4	9
Puristus poikittain lappeellaan	$f_{c,90,MLA}$	1,8	1,0	2,2
Leikkaus syrjällään	$f_{v,k}$	4,1	2,4	4,5
Lappeellaan pintaviilin suuntaan	$f_{v,k}$	2,3	1,3	1,3
<b>Jäykkyysominaisuudet (N/mm<sup>2</sup>)</b>				
Kimmomoduli	$E_{mean}$	13800	10000	10500
Liukumoduli	$G_{edge, mean}$	600	400	600
<b>Tiheydet (kg/m<sup>3</sup>)</b>				
Ominaisihteys	$\rho_k$	480	410	480
Tiheyden keskiarvo	$\rho_{mean}$	510	440	510

Taulukko 3.4 - Kerto-S, Kerto-T ja Kerto-Q LVL:n ominaislujuudet, kokovaikutuseksponentit, jäykkyysominaisuudet ja tiheydet (VTT Certificate No 184/03 ja sertifikaatti VTT-C-1781-21-07).

(PUUINFO, 2020, p. 18)

Materiaali	Käyttöluokka	Kuorman aikaluokka		
		Pysyvä	Keskipitkä	Hetkellinen
Sahatavara, Pyöreä puutavara, Liimapuu, LVL, Vaneri, CLT	1	0,60	0,80	1,10
	2	0,60	0,80	1,10
	3	0,50	0,65	0,90
Lastulevy P4 <sup>0</sup> , OSB/2 <sup>0</sup> , Kova kuitulevy	1	0,30	0,65	1,10
	2	0,20	0,45	0,80
Lastulevy P6 <sup>0</sup> , OSB/3 ja OSB/4	1	0,40	0,70	1,10
	2	0,30	0,55	0,90
Puolikovat kuitulevyt: MBH.LA <sup>0</sup> , MBH.HLS, MDF.LA <sup>0</sup> ja MDF.HLS	1	0,20	0,60	1,10
	2	-	-	0,80

Taulukko 3.1 - Muunnoskerroimen  $k_{mod}$  arvot.

<sup>0</sup> Saadaan käyttää vain käyttöluokassa 1

(PUUINFO, 2020, p. 17)

Figure 14. LVL analysis, page 5.

Lujuusominaisuuden mitoitusarvo  $X_d$  lasketaan seuraavasti:

$$X_d = k_{mod} \frac{X_k}{\gamma_M} \quad (2.12)$$

missä

$X_k$  on lujuusominaisuuden ominaisarvo

$\gamma_M$  on materiaaliominaisuuden osavarmuusluku (ks. taulukko 2.7)

$k_{mod}$  on muunnoskerroin, jonka avulla otetaan huomioon kuorman keston ja kosteuden vaikutus (ks. taulukko 3.1)

Perusyhdistelmät:	
Sahatavara ja pyöreä puutavara yleensä	1,3
Liimapuu, CLT	1,25
LVL, vaneri, OSB-levy	1,2
Muu lastulevy, kuitulevyt	1,3
Liitokset	1,3
Onnettomuusyhdistelmät	1,0

Taulukko 2.7 - Suomessa käytettävät materiaalien osavarmuusluvut  $\gamma_M$

(PUUINFO, 2020, p. 15)

(PUUINFO, 2020, p. 15)

$$k_h := \min \left( \left( \frac{300}{2725} \right)^{0.12}, 1.2 \right) = 0.767 \quad ((3.1), \text{Taulukko 3.4})$$

$$f_{mk} := 32 \text{ MPa} \quad (\text{Taulukko 3.4})$$

$$k_{mod} := 0.8 \quad (\text{Taulukko 3.1})$$

$$\gamma_M := 1.2 \quad (\text{Taulukko 2.7})$$

$$f_{md} := k_{mod} \cdot \frac{(k_h \cdot f_{mk})}{\gamma_M} = 16.371 \text{ MPa} \quad (2.12)$$

$$\sigma_m := \frac{M_{max}}{W} = 1.554 \text{ MPa}$$

$$\sigma_m < f_{md} \quad \text{OKAY!!!}$$

Max deflection verification (SLS)

$$\Delta_{max} := \frac{(R_{2SLS} \cdot L^3)}{48 \cdot E \cdot I} = 0.275 \text{ mm}$$

$$\Delta_{lim} := \frac{L}{300} = 20.567 \text{ mm}$$

$$\Delta_{max} < \Delta_{lim} \quad \text{OKAY!!!}$$

Figure 15. LVL analysis, page 6.

Smallest allowable height of 40mm LVL beam

$$h_{\min} := \sqrt{\frac{(6 \cdot M_{\max})}{b_{LVL} \cdot f_{md}}} = 839.661 \text{ mm}$$

$$b_{LVL} := 40 \text{ mm}$$

$$E := 10500 \frac{\text{N}}{\text{mm}^2} \quad I := \frac{(b_{LVL} \cdot h_{\min}^3)}{12}$$

Max deflection verification (SLS)

$$\Delta_{\max} := \frac{(R_{2SLS} \cdot L^3)}{48 \cdot E \cdot I} = 9.399 \text{ mm}$$

$$\Delta_{\text{lim}} := \frac{L}{300} = 20.567 \text{ mm}$$

$$\Delta_{\max} < \Delta_{\text{lim}} \quad \text{OKAY!!!}$$

Resistance of smallest allowable height LVL beam

$$b_{LVL} := 40 \text{ mm} \quad h_{LVL} := 840 \text{ mm}$$

$$E := 10500 \frac{\text{N}}{\text{mm}^2} \quad I := \frac{(b_{LVL} \cdot h_{LVL}^3)}{12}$$

$$W := \frac{(b_{LVL} \cdot h_{LVL}^2)}{6} = (4.704 \cdot 10^6) \text{ mm}^3$$

$$\sigma_m := \frac{M_{\max}}{W} = 16.358 \text{ MPa}$$

$$k_h := \min\left(\left(\frac{300}{840}\right)^{0.12}, 1.2\right) = 0.884 \quad ((3.1), \text{Taulukko 3.4})$$

$$f_{mk} := 32 \text{ MPa} \quad (\text{Taulukko 3.4})$$

$$k_{\text{mod}} := 0.8 \quad (\text{Taulukko 3.1})$$

$$\gamma_M := 1.2 \quad (\text{Taulukko 2.7})$$

$$f_{md} := k_{\text{mod}} \cdot \frac{(k_h \cdot f_{mk})}{\gamma_M} = 18.854 \text{ MPa} \quad (2.12)$$

$$\sigma_m < f_{md} \quad \text{OKAY!!!}$$

### 3.3.1 Results

Initial analysis of the LVL showed that a solid LVL wall 40mm wide and 2725mm high would be sufficient for carrying the external loads from the CLT, concrete and live loads. Also, the minimum height of LVL required to support the loads in case of a full-span opening was found to be 840mm.

## 4 Analysis Using Structural Design Software (RFEM)

The next phase of analysis involved modelling the structure in RFEM. First, a verification of the manual calculations was conducted. A model was made in with the LVL as a beam member. After an initial simplified analysis was conducted, it was found that treating the LVL as a beam member caused discrepancies in the model. A surface model was then created and found to be a more accurate representation of the structure. Next, detailed models treating the LVL as both a member and a surface were made. The purpose of these models was to compare ways of modelling the structure and find out how the overall behaviour of the structure is affected. To get these models to work, extensive trouble shooting was required. Once the models were successful and the hand calculations were verified, the surface model was found to be most reliable and useful. The surface model was developed further by adding a series of rigid bars to simulate the sylomer pads and analyse the effects of different hinge configurations. Finally, simplified models were created where the actual material properties of the sylomer pads were used to find the correct dimensions and best contact points in design scenarios with a solid wall and a wall with openings.

## 5 Simplified Models to Verify Manual LVL Calculations

In the first model created for analysis of the structure with RFEM, the LVL was treated as a beam. The purpose of this model was to verify the manual calculations of the force from the CLT and concrete on the LVL (see Fig. 10 through 14). A simplified model was created applying the same loading as from the hand calculations, and a error was found in the results for the reaction force at midspan (R2). Through troubleshooting, it was found that by changing the beam to a typical RHS profile, the results matched the manual calculations more precisely (see Fig. 16 and 17 below).

Figure 16. Error in reaction at midspan (R2) with LVL modeled as a beam.

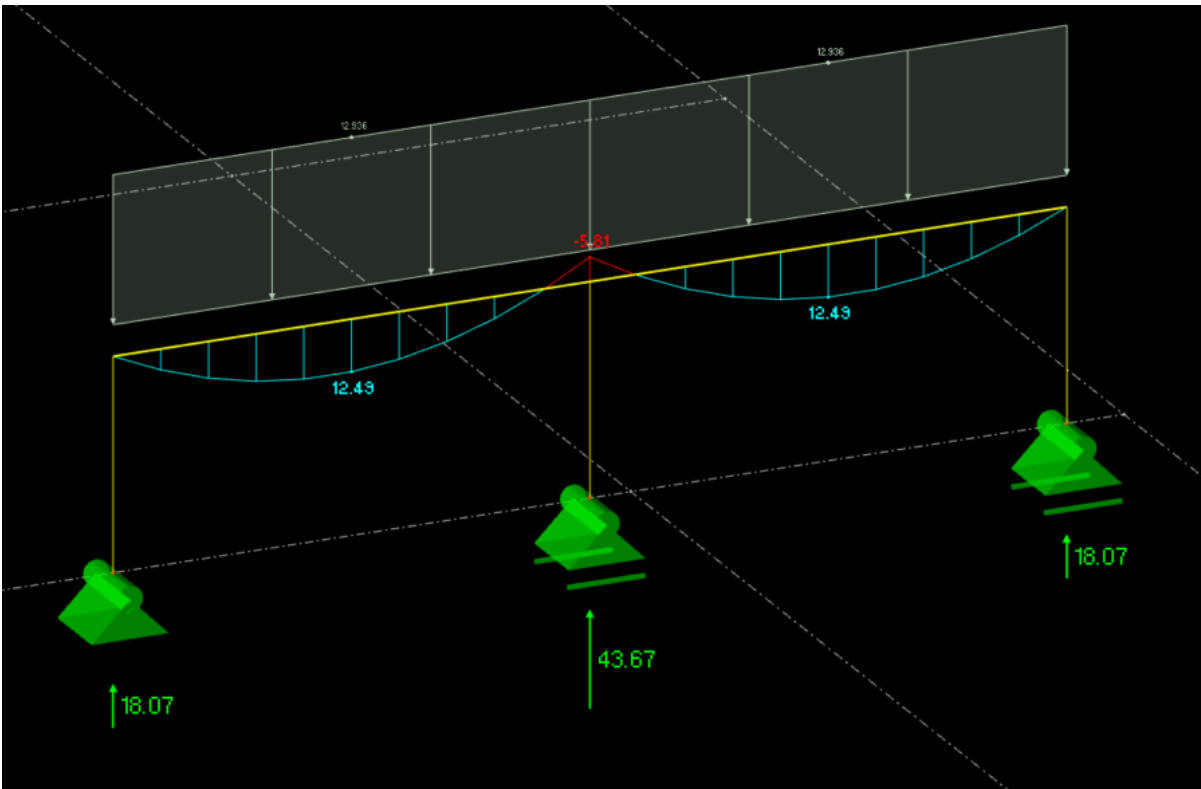
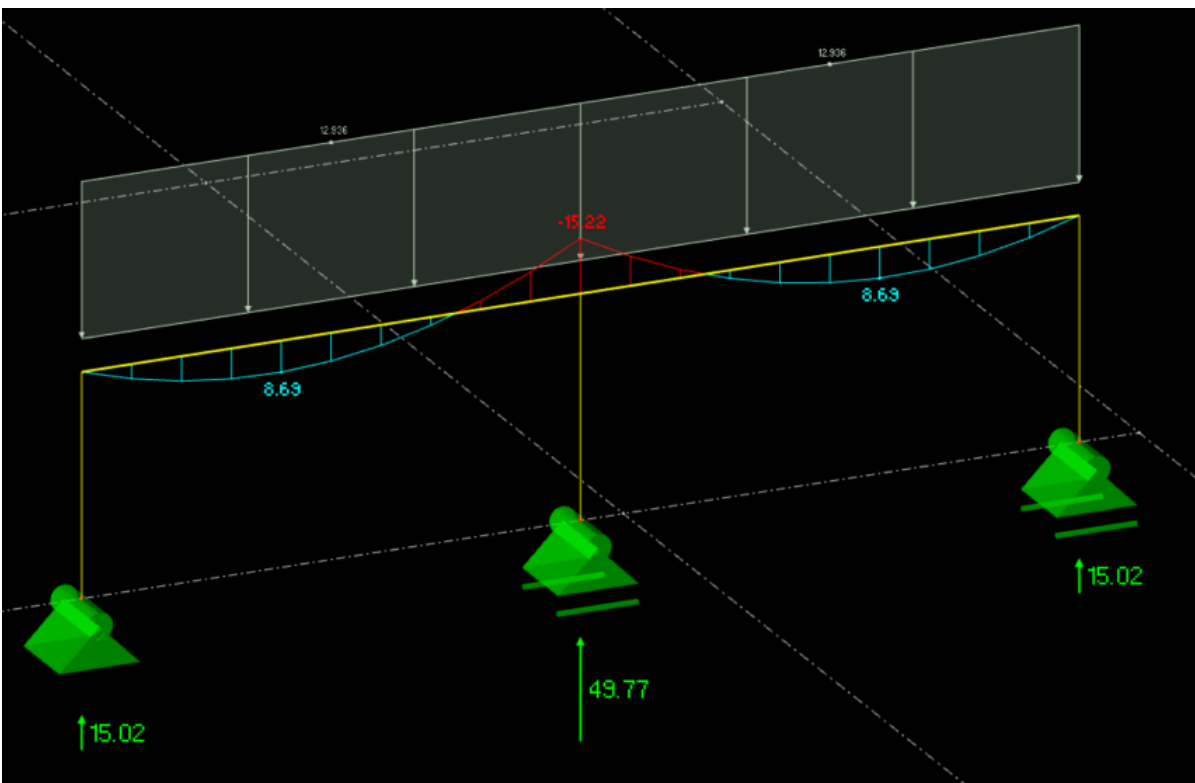


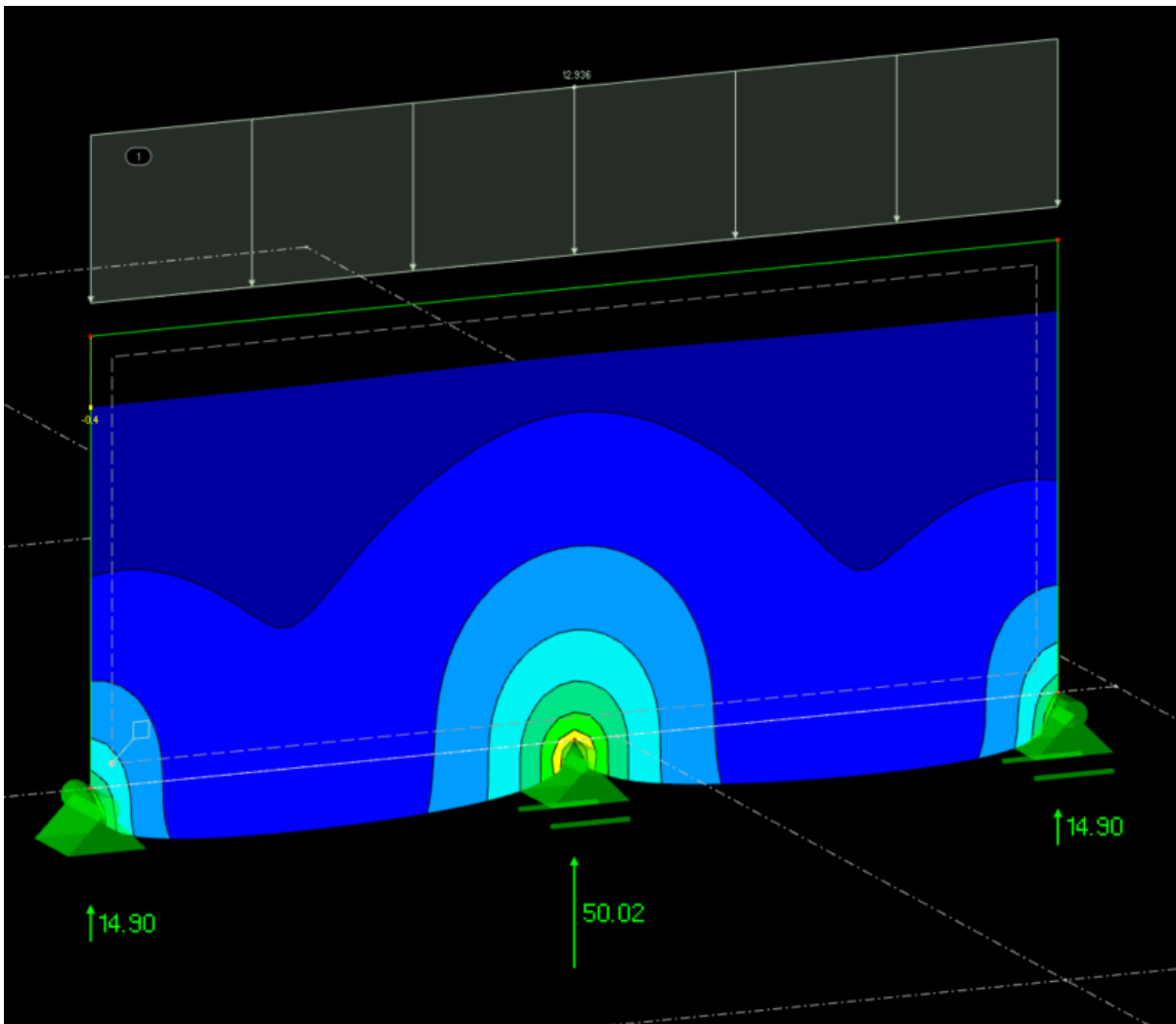
Figure 17. Correct results with RHS beam.





Continuing the analysis, a simplified model was created in which the LVL was represented as a surface. The results for R2 in this model were also verified to fit the manual calculations more precisely. The reason for the error in the results was therefore found to be a result of modelling the LVL as a member in RFEM.

Figure 18. Correct results with LVL as a surface.



Next, the force R2 was applied to the simplified models to check the maximum moment and deflection of the LVL from the manual calculations. The results for the maximum moment and deflection were verified in the beam member model, and the maximum deflection was verified in the surface model (see figures below).

Figure 19. Maximum bending moment verified in the LVL beam member model.

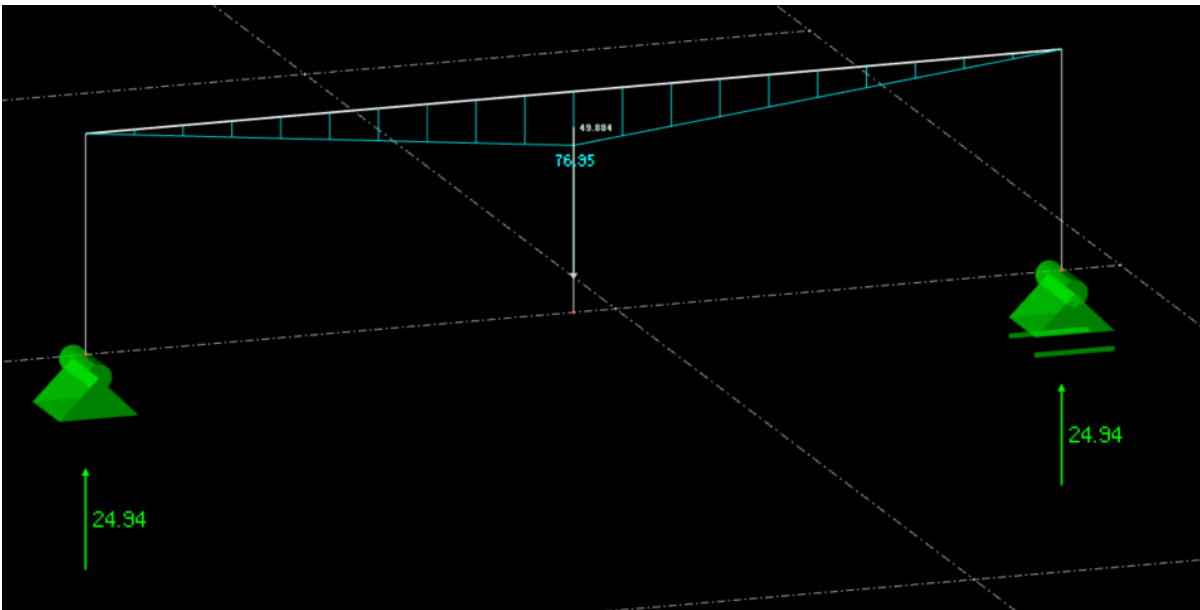


Figure 20. Maximum deflection verified in the LVL beam member model.

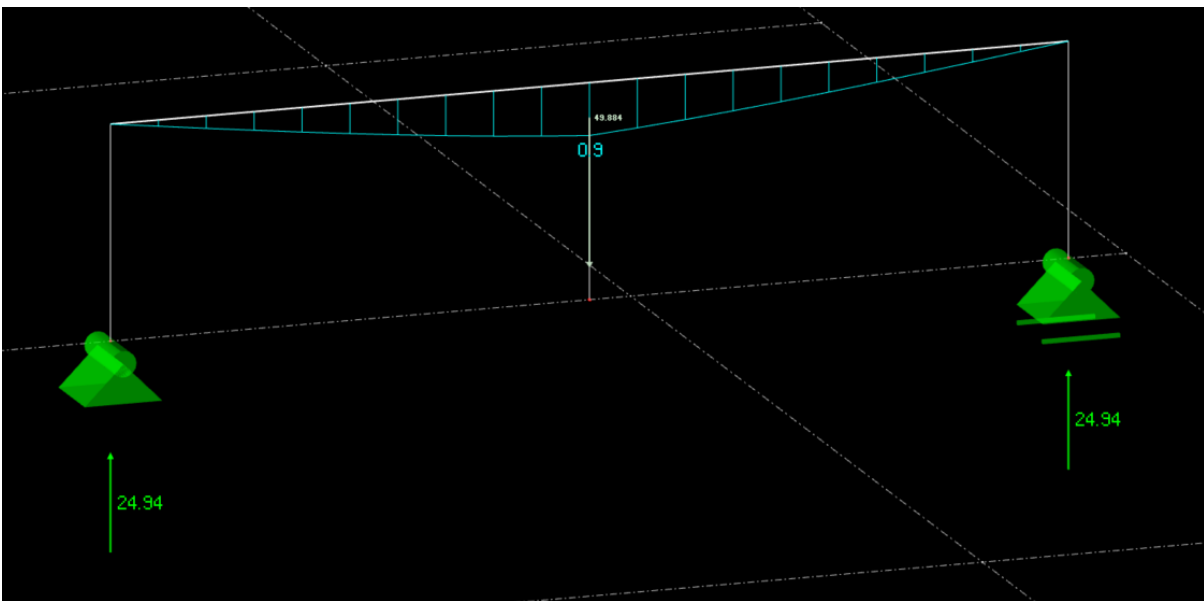
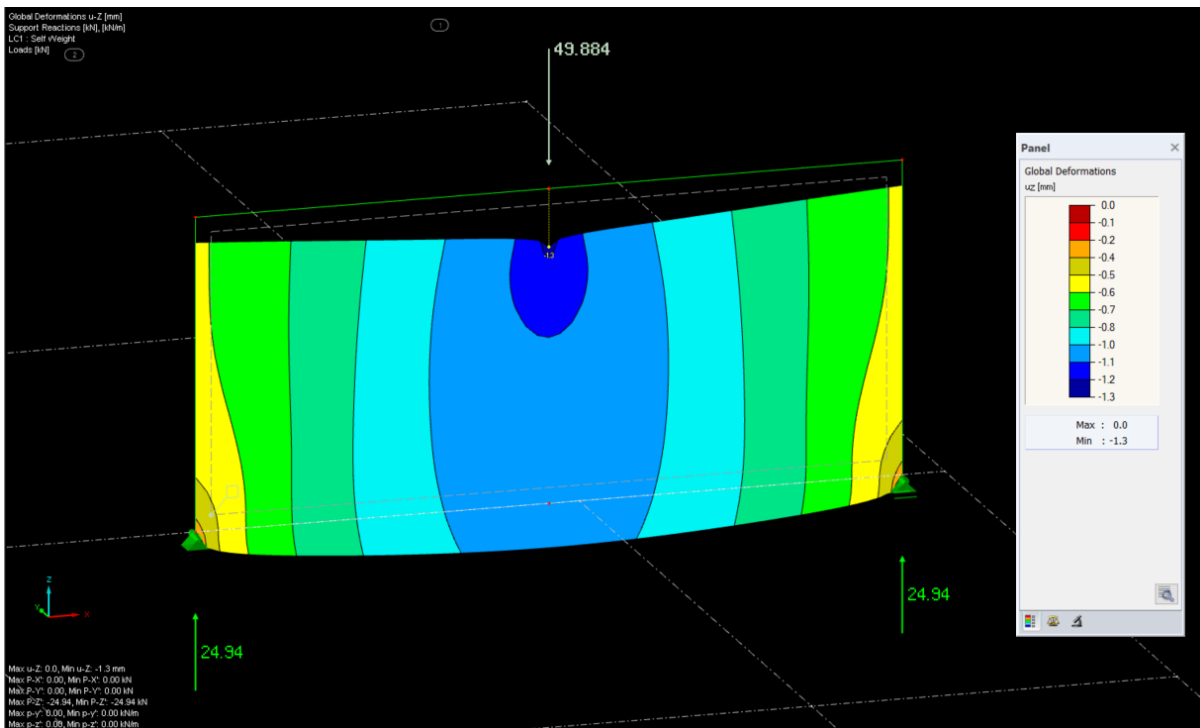


Figure 21. Maximum deflection verified in surface model.



## 5.1 Results

An error was found in the member model when verifying the load caused by the CLT and concrete acting on the LVL. This error was corrected by modelling the LVL as a surface. The member model was successful in verifying the maximum moment and deflections, and the surface model was successful in verifying the deflections. The manual calculations were therefore found to be accurate. Also, while both ways of modelling the structure were found to be accurate and useful, the error found in the member model indicates that modelling the LVL in RFEM as a surface may be more reliable.

## 6 Detailed Models to Analyse the Behaviour of the Structure

Due to the variation in the results of the member model as compared to the surface model, it was decided to make more developed models where the LVL is treated first as a member, then as a surface. A comparison between the behaviour and calculation results of the structures was then made, to find the most appropriate way to model the structure. After the surface model was found to be more reliable, a comparison of hinge configurations was then made.

## 6.1 Detailed Model with LVL as a Member

To model the geometry of the design with members, the vertical LVL surfaces were idealized as columns and horizontal parts of the surfaces over the windows and doors were modelled as beams. The horizontal parts of the surfaces below windows were not designed to carry loads, so they were left away from the model. In order to achieve the correct geometry of the timber units and connect the ends of the members together, rigid connections were used (see Fig. 22).

Figure 22. RFEM settings for the LVL as a beam member.

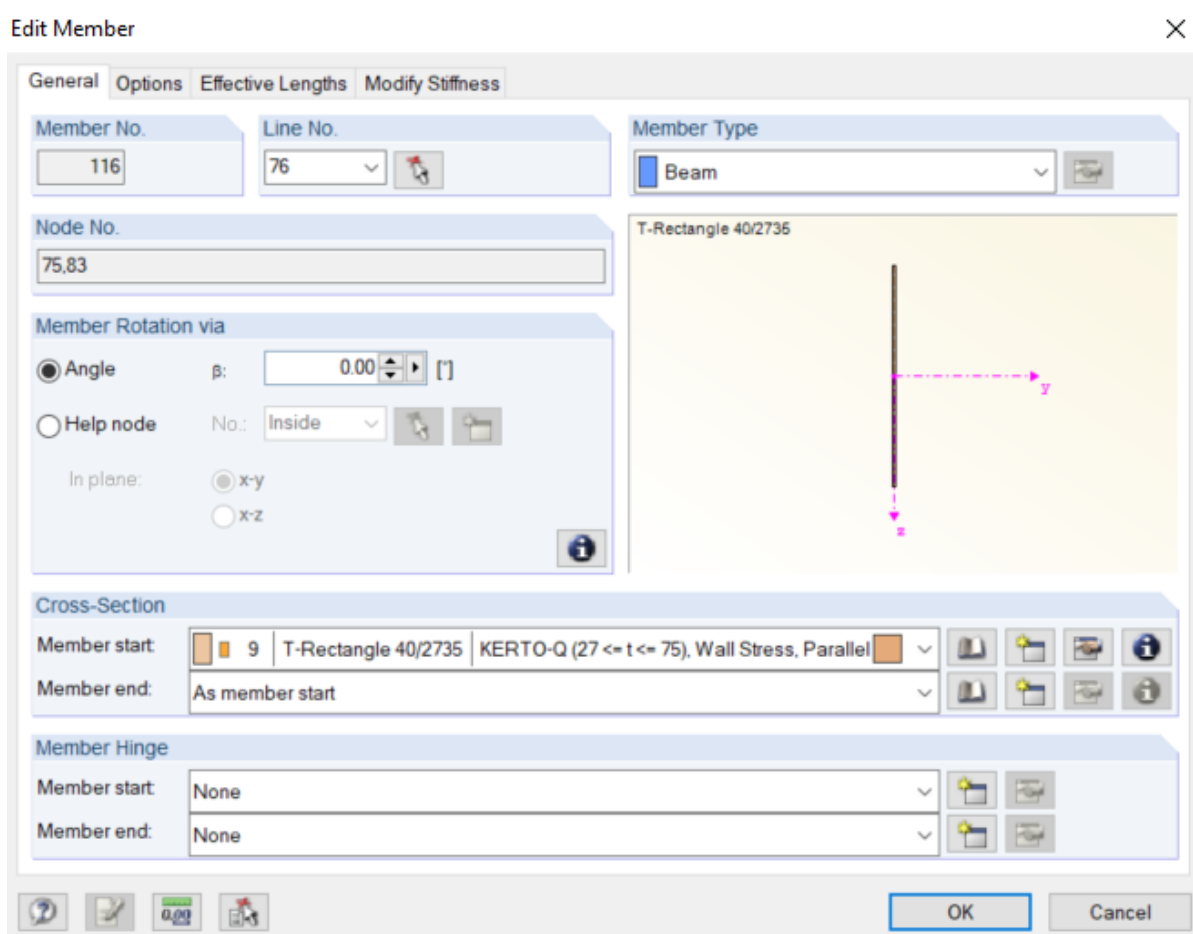
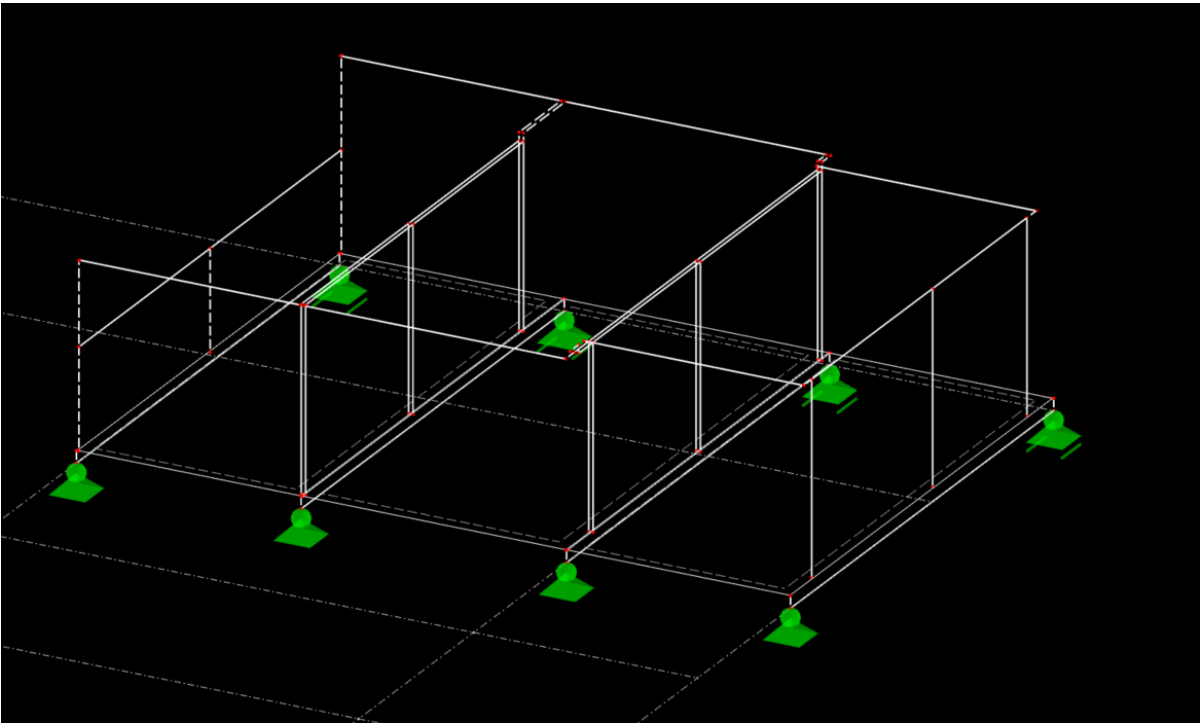


Figure 23. Early phase of the LVL beam member model.



During the early phase of the modelling, it was realized that to represent the behaviour of the structure accurately, the ceiling surfaces had to be left away from the model. The reason for this was that with these surfaces modelled, the units would behave as beams with the CLT ceiling acting as a flange. Since the design did not take these surfaces into account as primary load-bearing elements, they could not be allowed to take loads in the model. So, to get the model to behave as a one-way slab supported by LVL beams, the ceilings were represented as imposed dead weight line loads acting along the tops of the members. As a result of leaving these elements away, the stability of the structure was lost in the model. Therefore, to simulate the real-world stability, tension members were used on the side walls and nodal supports preventing movement along the x and y axes were used at the top of the members (see figures below).

Figure 24. The LVL beam member model with tension members and nodal supports.

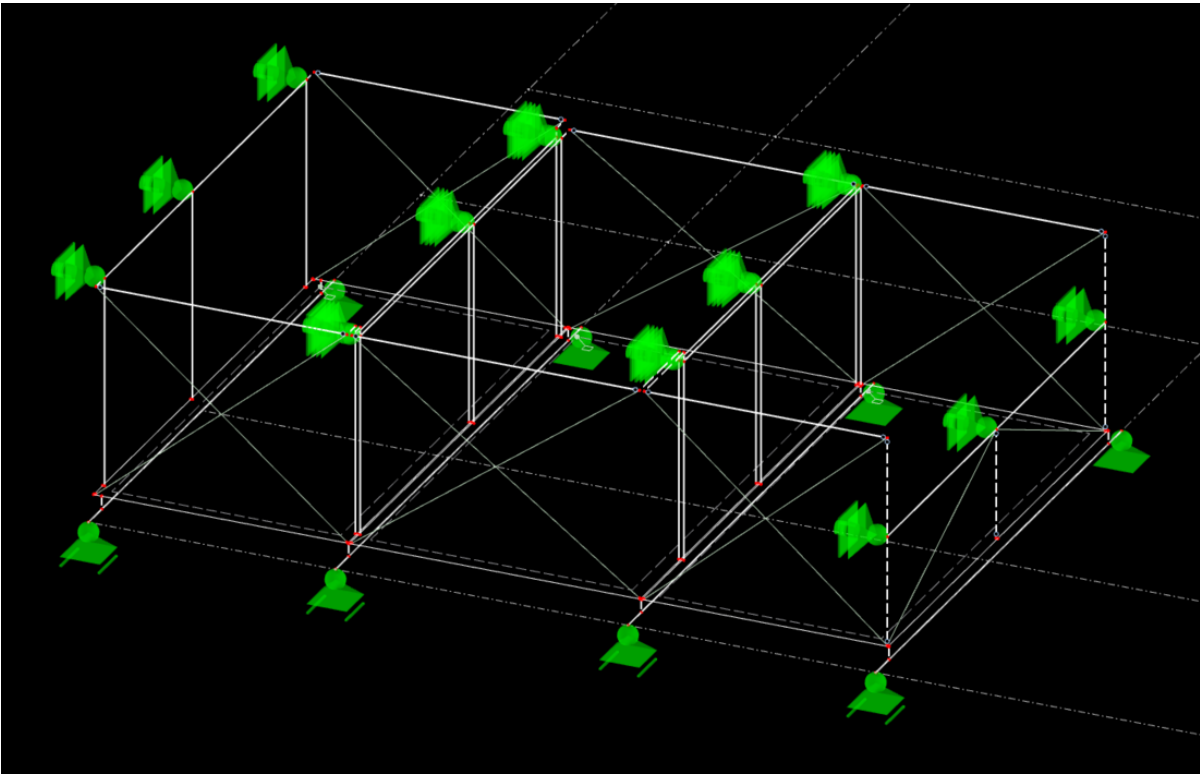
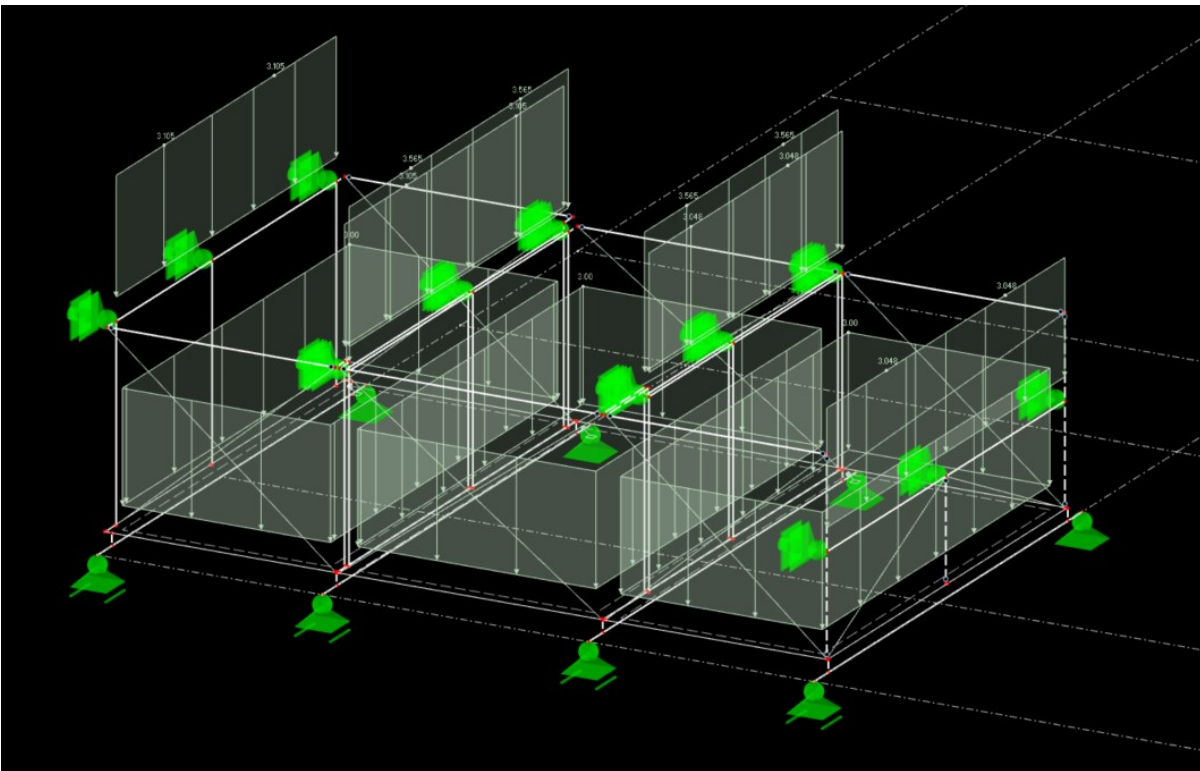


Figure 25. The LVL beam member model with loads.



After inputting the loads from the CLT as line loads acting along the top of the members and attempting to calculate the model, instability was found in the concrete surfaces. Finding a solution to the instability was difficult and required extensive troubleshooting. After altering supports and hinges in various ways and not finding a solution, advice from experienced engineers working at the company was given. First, couple members rigid-rigid were added to connect vertical members to the slabs. Then, the surface mesh for the concrete slabs was refined. After these changes did not solve the instability, the model was regenerated with a higher tolerance of 0.5mm for standard nodes and generated nodes. With this modification, the model was finally calculated successfully (see figures below).

Figure 26. Coupling rigid-rigid connection to slab added.

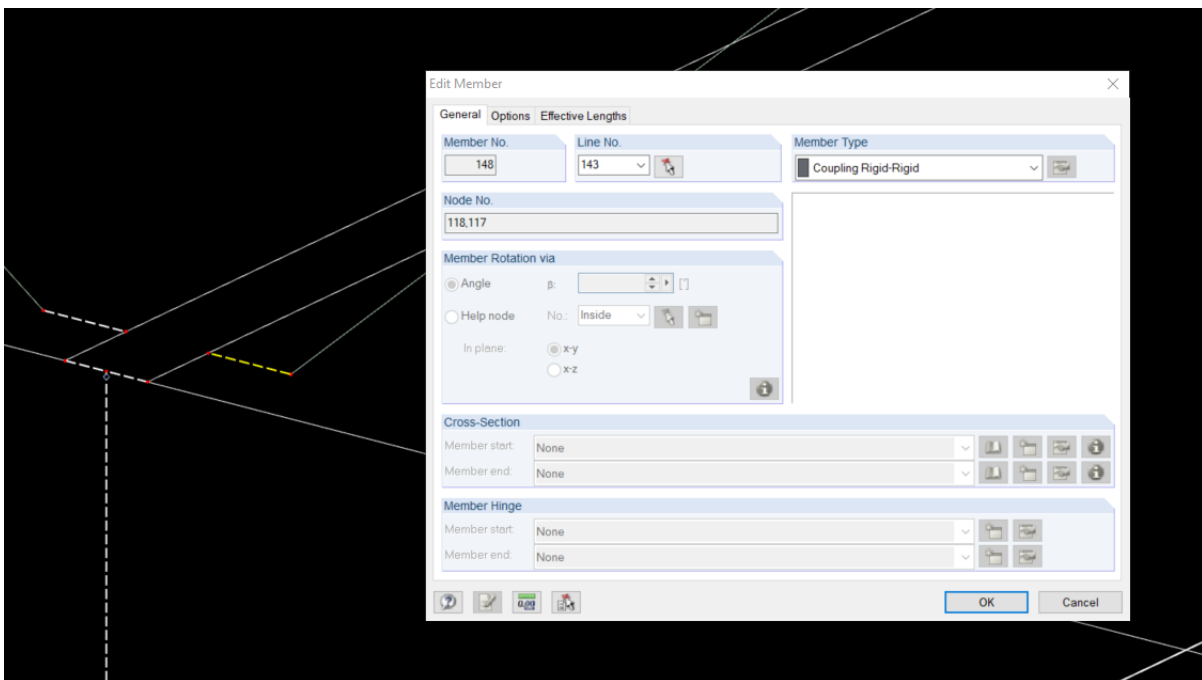


Figure 27. Mesh refinement settings.

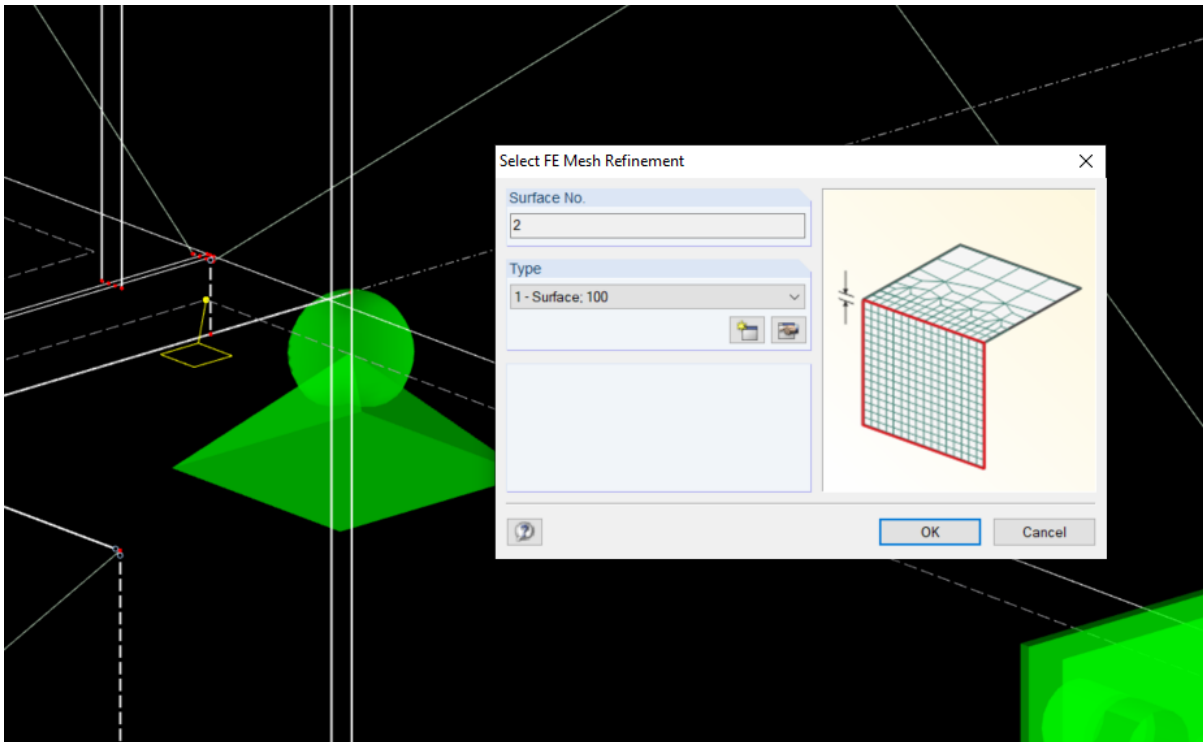
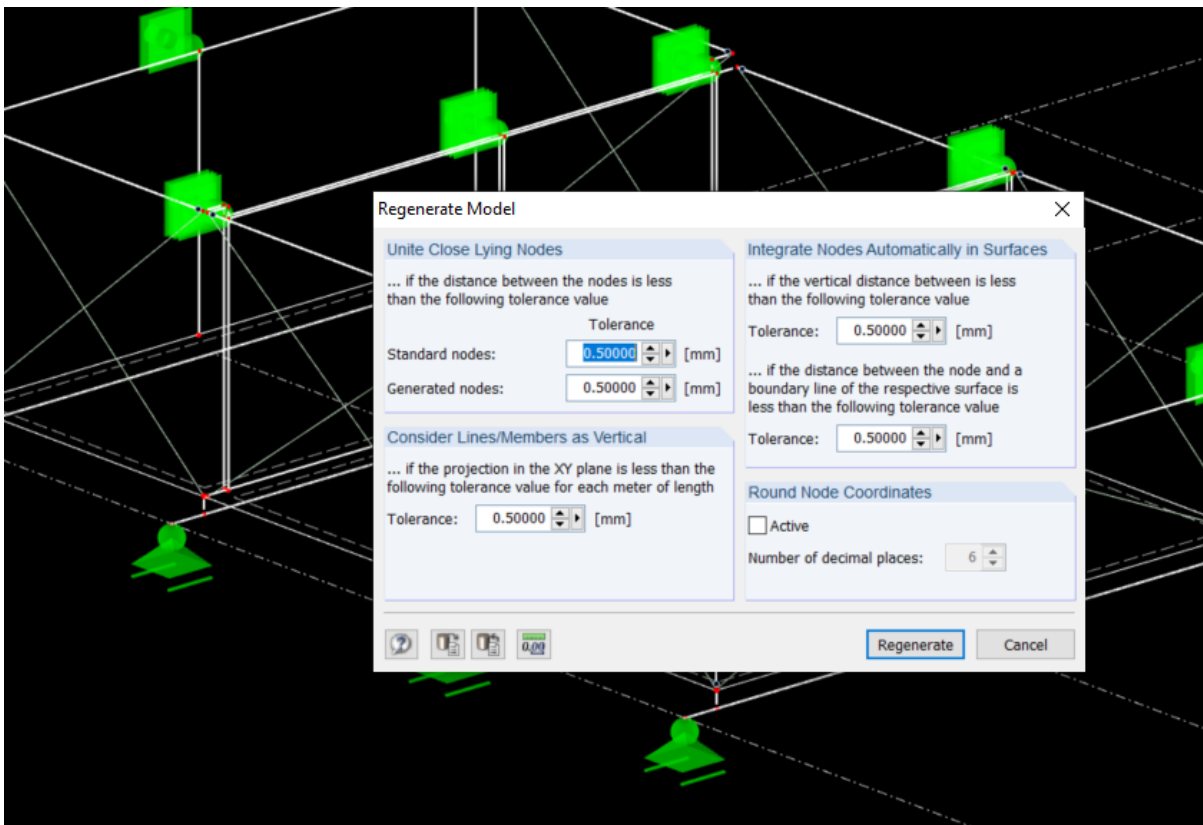


Figure 28. Regenerate model settings.





### 6.1.1 Results

The maximum bending moment of the solid wall according to RFEM was found to be 69.25 kNm. According to the manual calculations laid out above, the maximum bending moment was found to be 76.9 kNm. Given that in the model, all the openings are taken into account, the loads would then be smaller, so the discrepancy is reasonable. The deflection of the solid wall was found to be about 2 mm more than in the hand calculations, and 1.5 mm more than in the simplified model. While differences would be expected from the surfaces being divided into members and connected through midpoints, the overall behaviour of the structure was reasonable.

Figure 29. Maximum bending moment in member model verified.

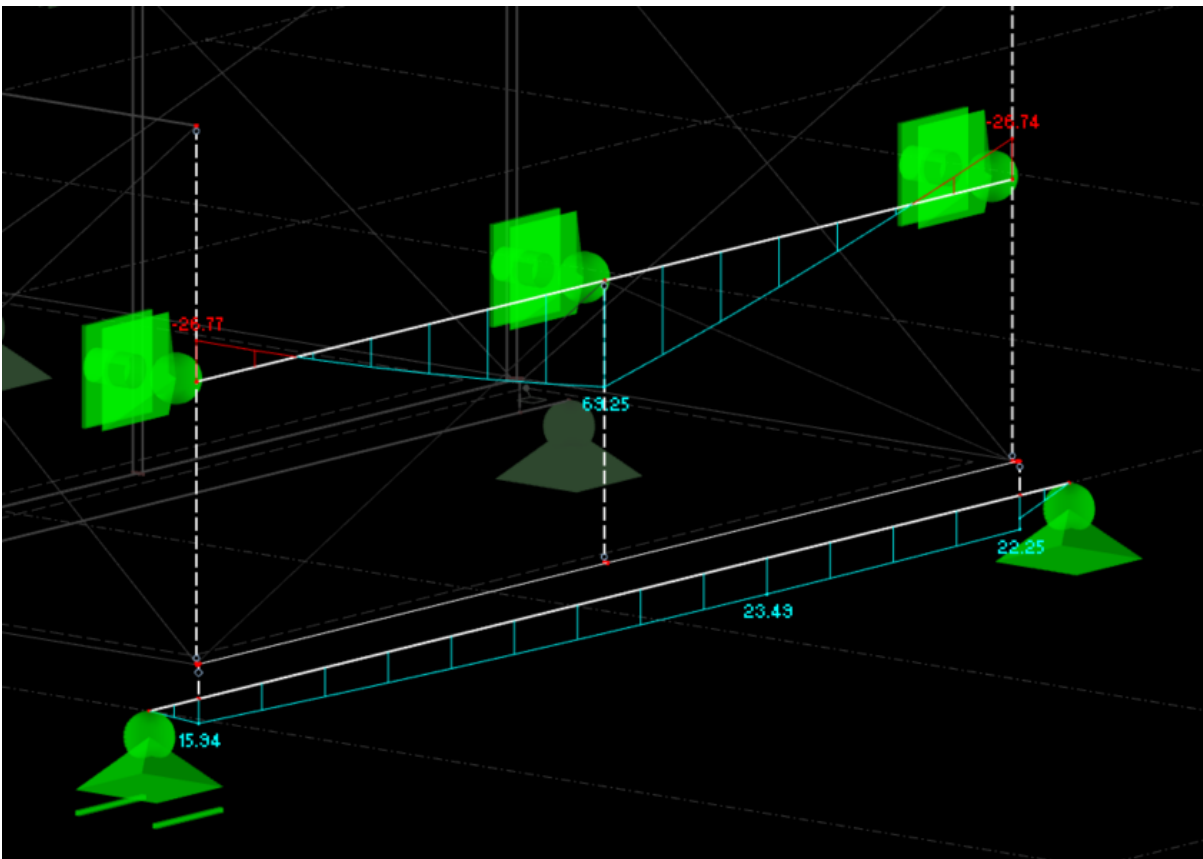


Figure 30. Deflection of LVL in member model verified.

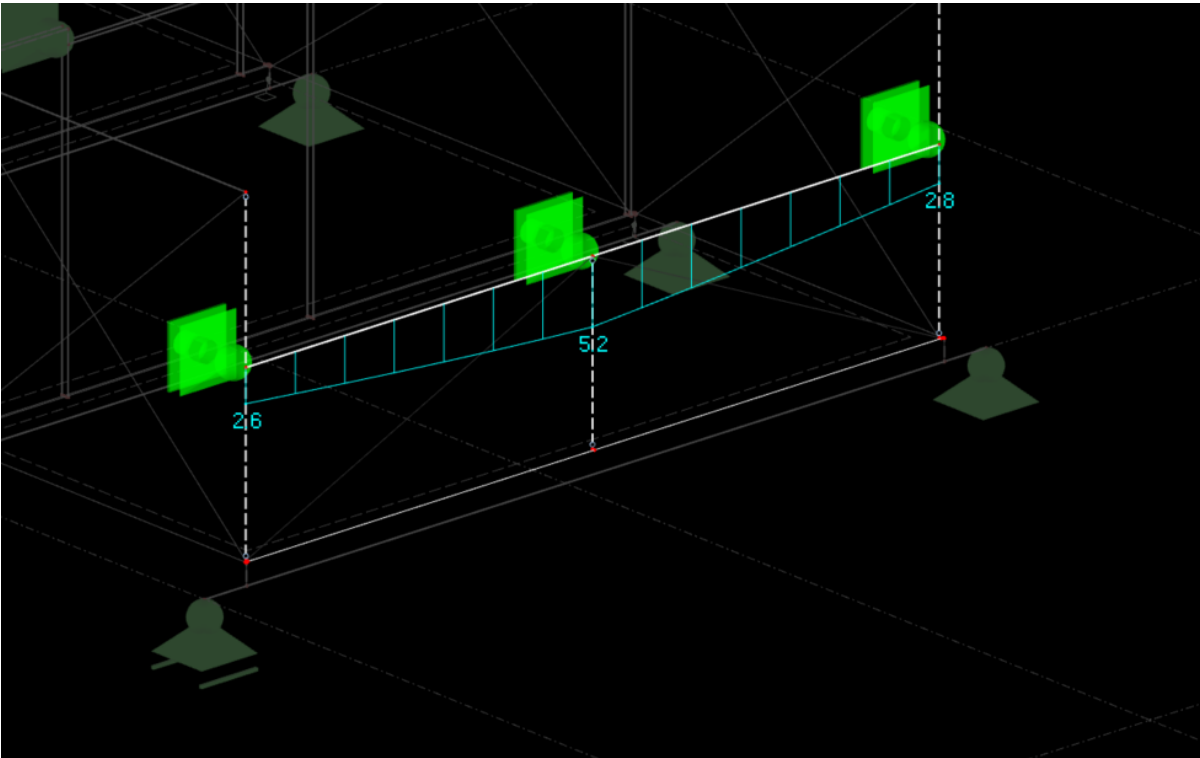
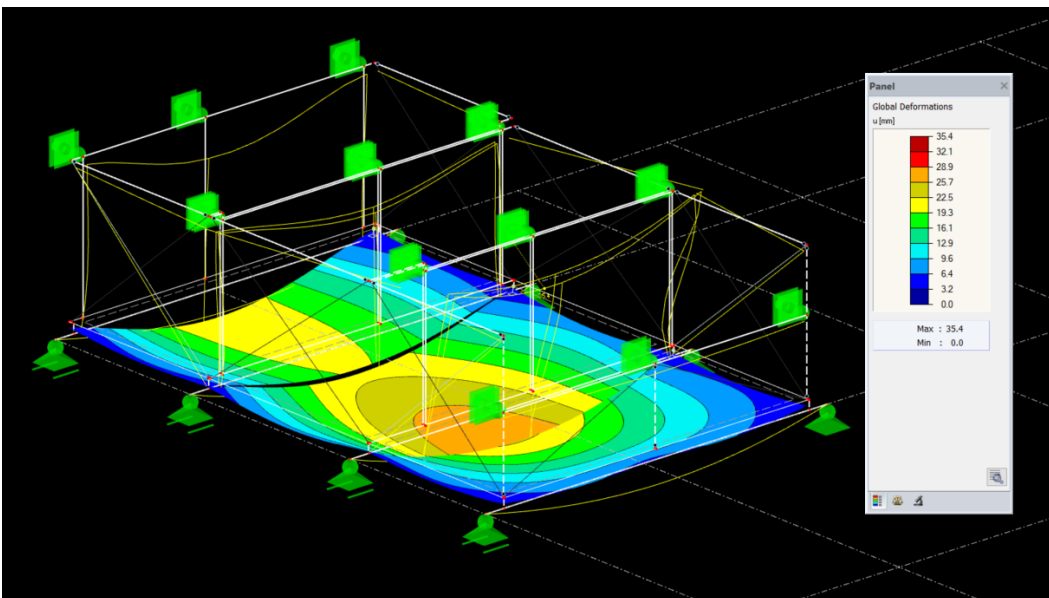


Figure 31. Global deformations  $u$  in member model.

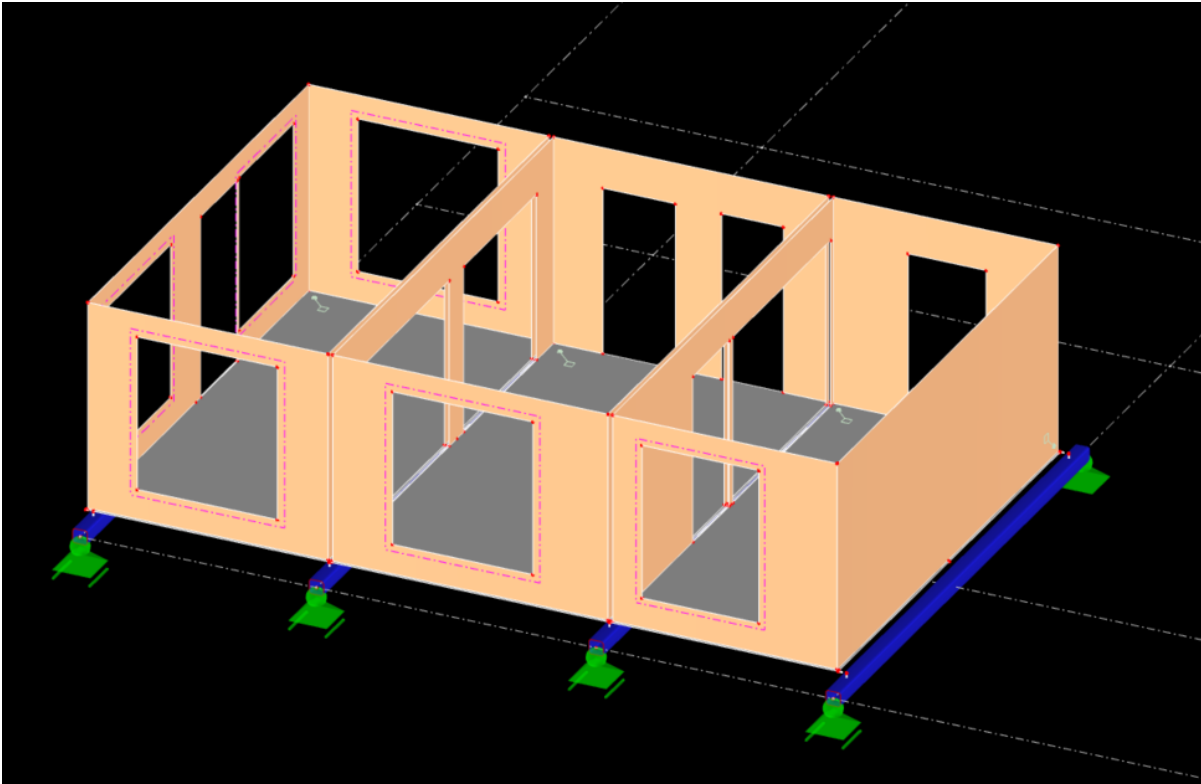


## 6.2 Detailed Model with LVL as a Surface

After successfully calculating the member model, all the LVL members were deleted and replaced by LVL surfaces. The LVL surfaces were modelled with openings according to the design of the

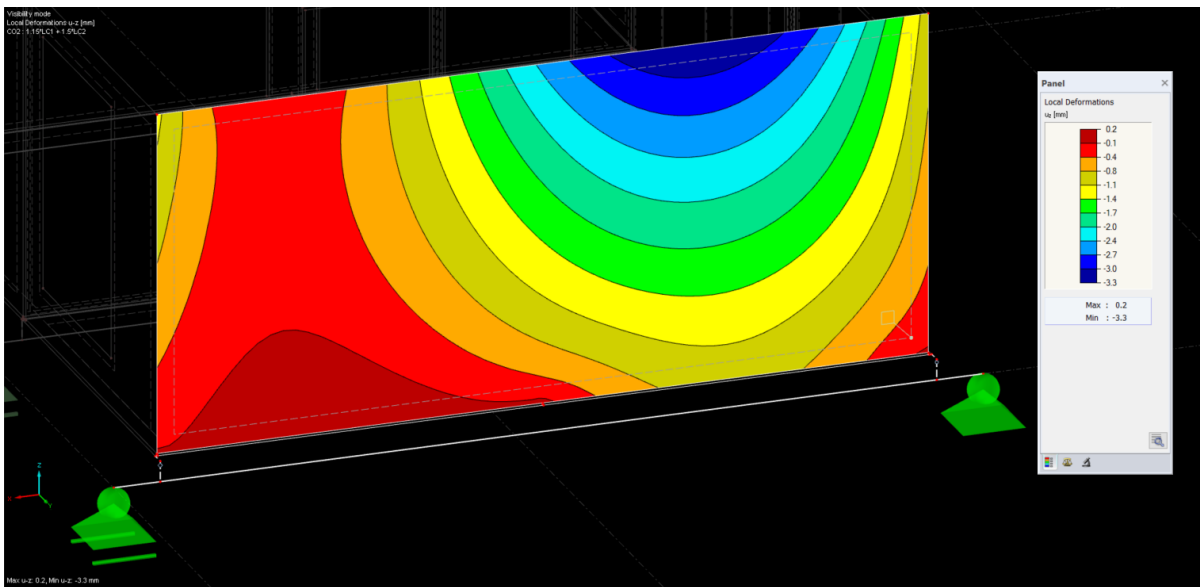
structure. In the preliminary model, the LVL was also connected to the concrete slabs along the same boundary lines. However, it was soon realized that to accurately represent the geometry of the structure, there would have to be a 10 mm gap between the LVL and concrete. The LVL surfaces were then raised 10 mm and the connection between the LVL and concrete slabs were made with steel bars representing the threaded bar connections in the design of the structure.

Figure 32. Surface model in solid display.



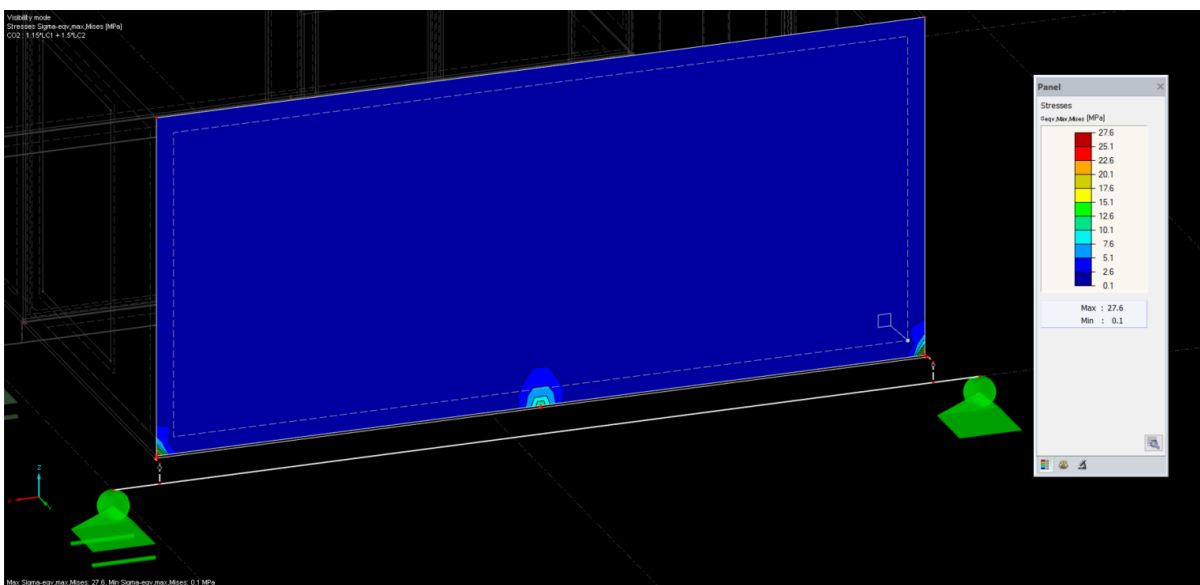
The loads were input, and the model was calculated successfully. The solid wall was found to be deflecting similar to the member model. However the location of the maximum local deformation  $u-z$  was not located in the centre of the LVL surface as expected.

Figure 33. Local surface deformations uz of LVL in surface model.



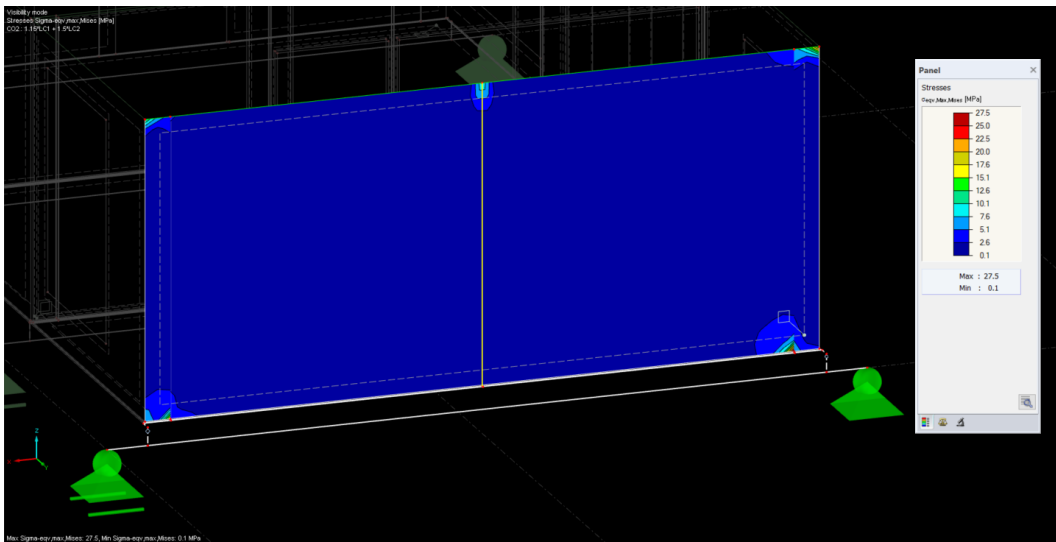
Further analysis of the stress ( $\sigma_{eqv,Max,Mises}$ ) showed that all of the stress was occurring in the bottom of the LVL surface. However, considering how the bars are connected to the actual structure, and how the concrete floor hangs from the centre bar-LVL connection, the stress would be expected to occur at the top of the centre of the LVL. Also, the locations of the threaded bars did not correspond to the actual locations in the structure. Therefore, the placement and connection points of the steel bars needed to be adjusted.

Figure 34. First results of  $\sigma_{eqv,Max,Mises}$  with incorrect location of stress in the center.



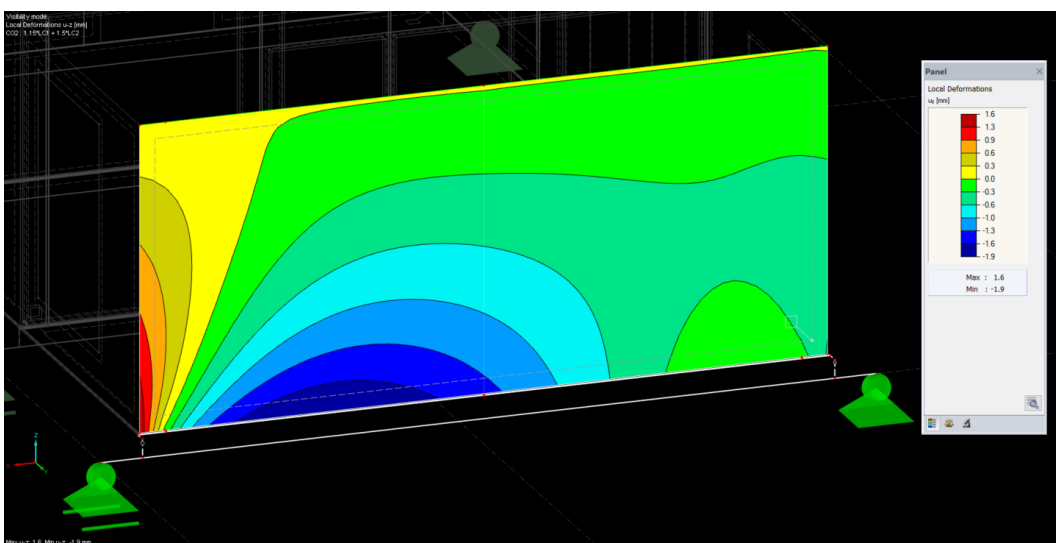
After making the adjustments to the locations, and moving the center steel bar connection to the top of the LVL, the stress ( $\sigma_{eqv,Max,Mises}$ ) was corrected.

Figure 35. Updated results of  $\sigma_{eqv,Max,Mises}$ .



The local deformations  $u-z$  were also affected by the change. The max deformation was still not occurring at exact midpoint of the solid wall, but it was much closer. An explanation for this is the asymmetry of the openings in the adjacent wall from the same module, therefore the location of the deformation is reasonable.

Figure 36. Local surface deformations  $u-z$ .



### 6.2.1 Results

Both the member model and surface model were found to be behaving reasonably and giving results which closely correspond to the hand calculations and simplified models. However, the surface model was found to give more reliable results which correspond more closely with the expected behaviour of the actual structure. Also, with the surface model, it was found to be easier to correctly model connections between the different materials, making it more useful in simulating and analysing them. Therefore, it was decided to use the surface model to make further analysis of the composite connections.

### 6.3 Analysis of Hinge Configurations in Detailed Surface Model

In the next phase of analysis, the surface model was developed further by adding a series of rigid connections to simulate the sylomer pads and test the effects of different hinge configurations on the behaviour of the structure. The location of the rigid bar series were centred directly below the threaded bar connections on the ends of the modules in order to distribute the loading straight down to the beam. No connections were made between the centres of the modules and the centres of the beams so that the maximum loading from the concrete will be hanging from the LVL. Three hinge configurations were tested: rigid, rotating, and sliding.

Figure 37. Series of rigid connections added to simulate sylomer pads with rigid hinges.

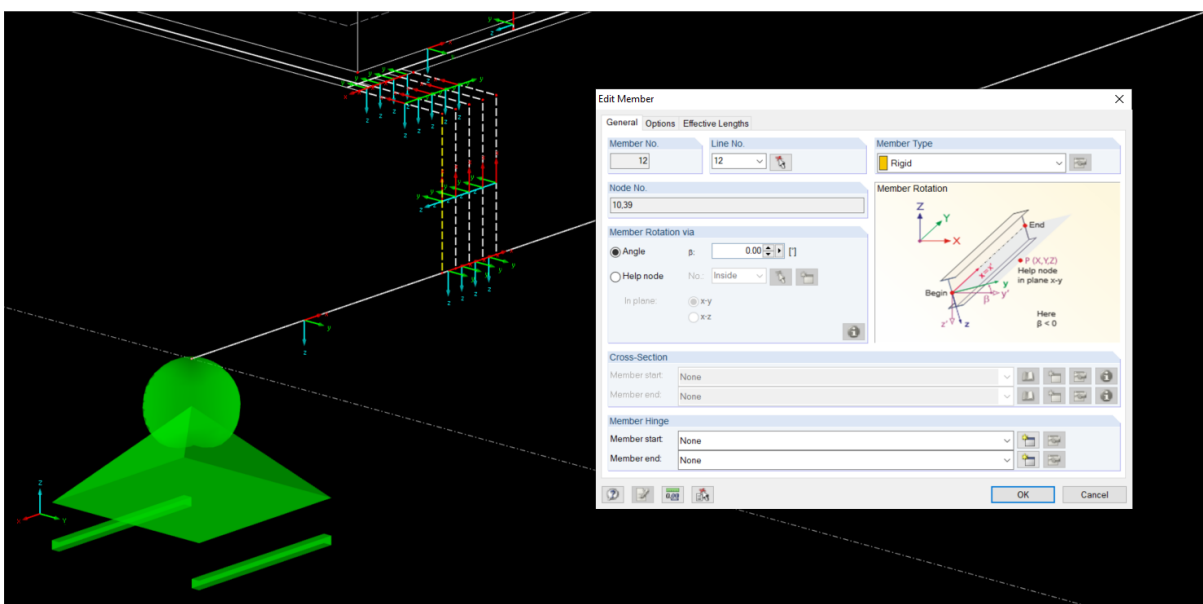


Figure 38. Series of rigid connections added to simulate sylomer pads with rotating hinges.

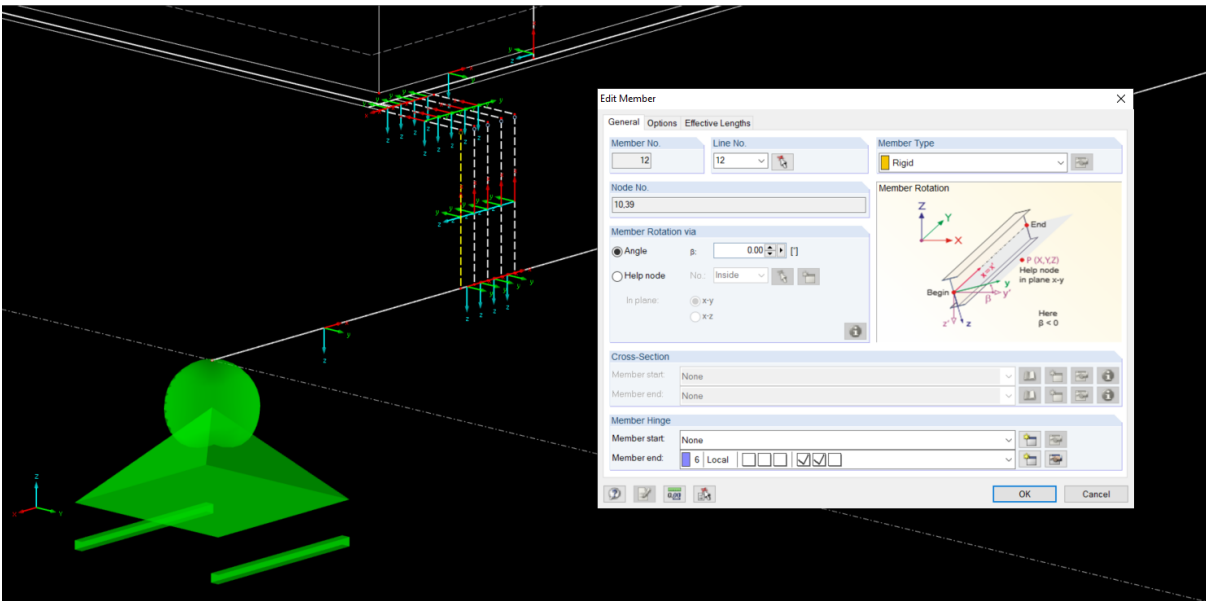


Figure 39. Series of rigid connections added to simulate sylomer pads with sliding hinges.

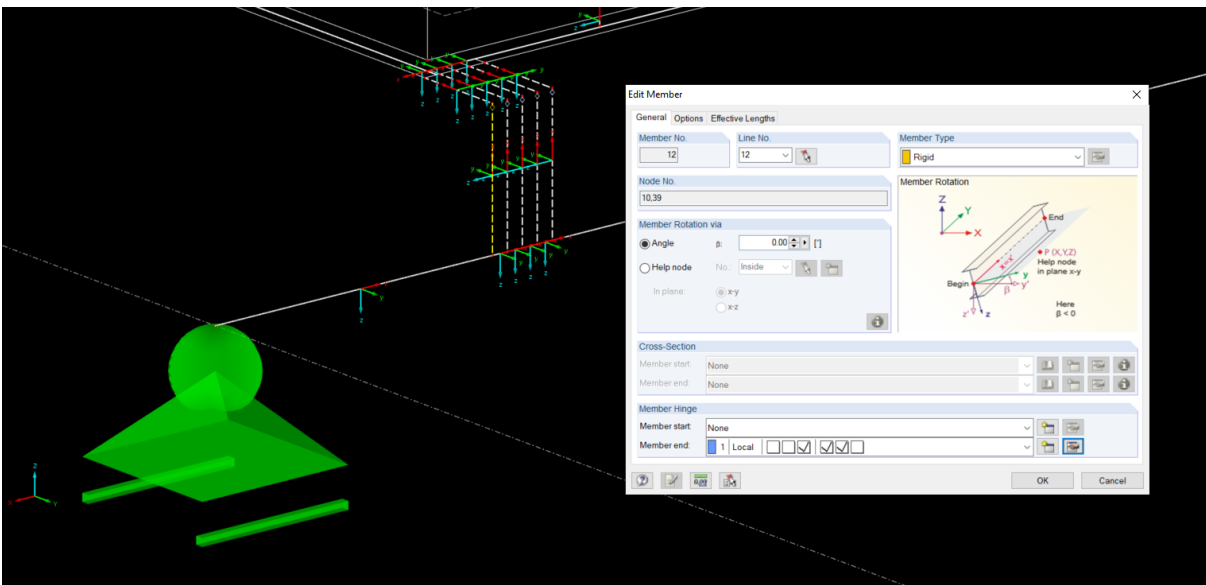


Figure 40. Global deflection in uz of structure with rigid hinges.

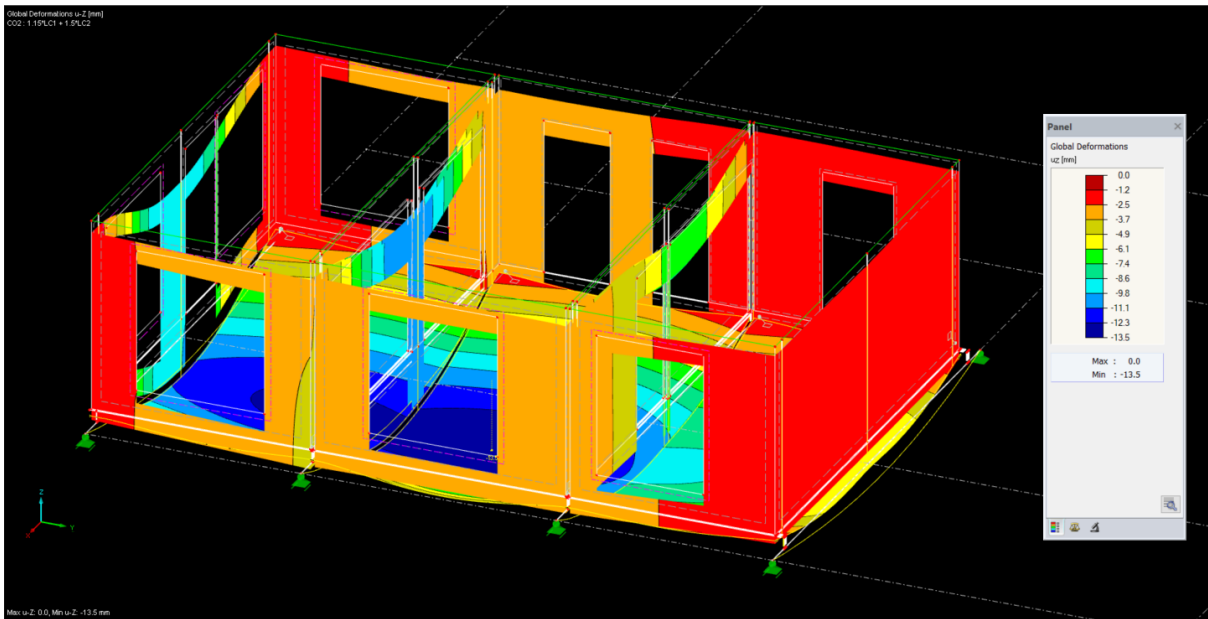


Figure 41. Global deflection in uz of structure with rotating hinges.

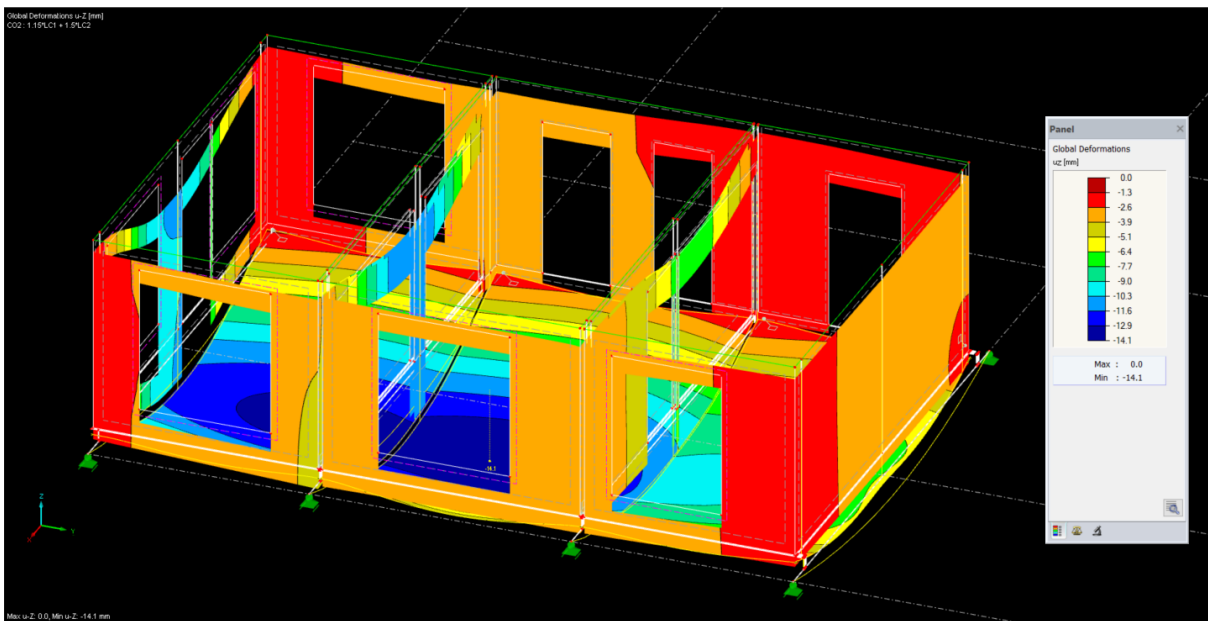




Figure 42. Global deflection in uz of structure with sliding hinges.

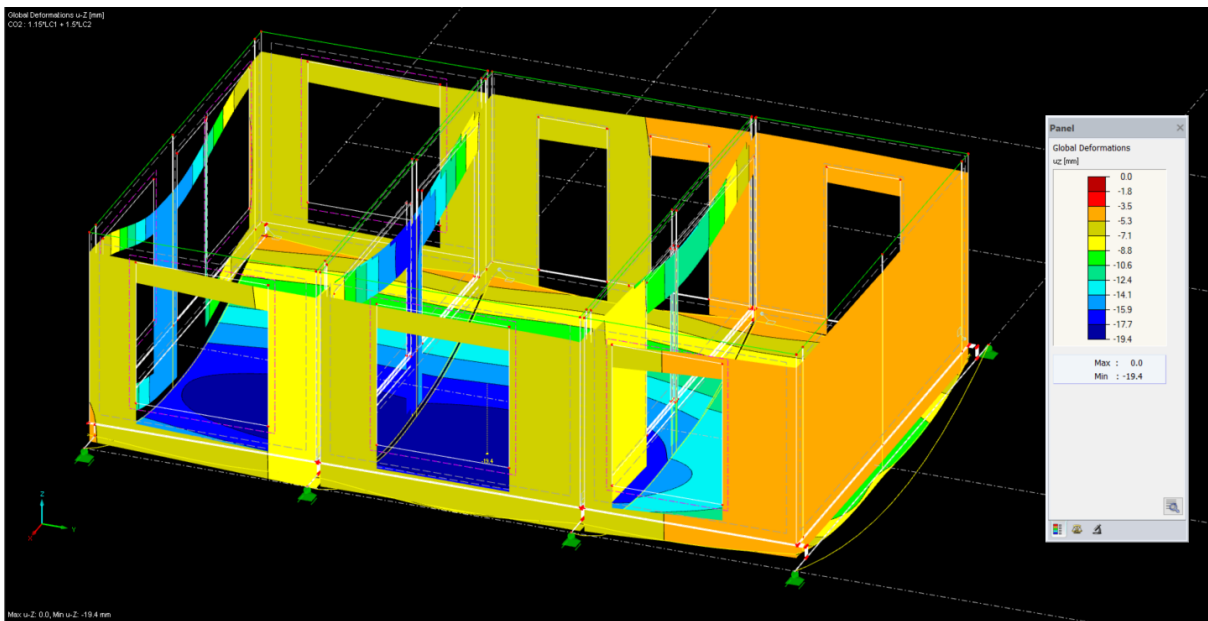


Figure 43. Local deflection of members in uz/uv with rigid hinges.

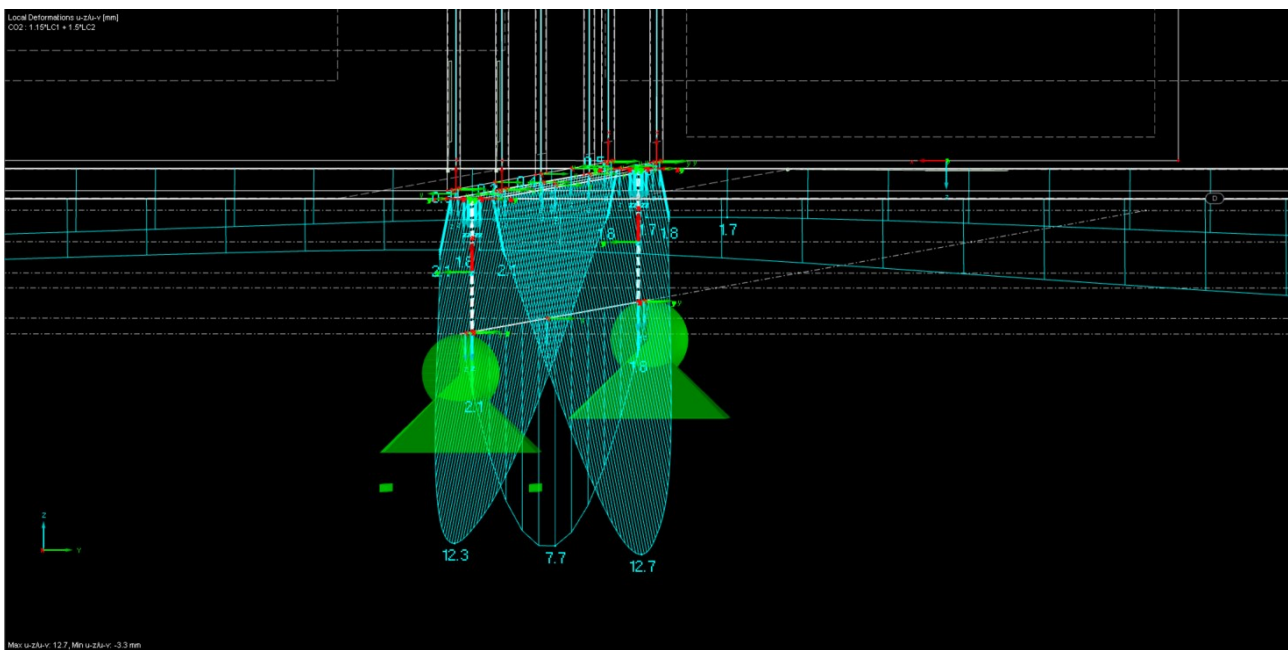


Figure 44. Local deflection of members in uz/uv with rotating hinges.

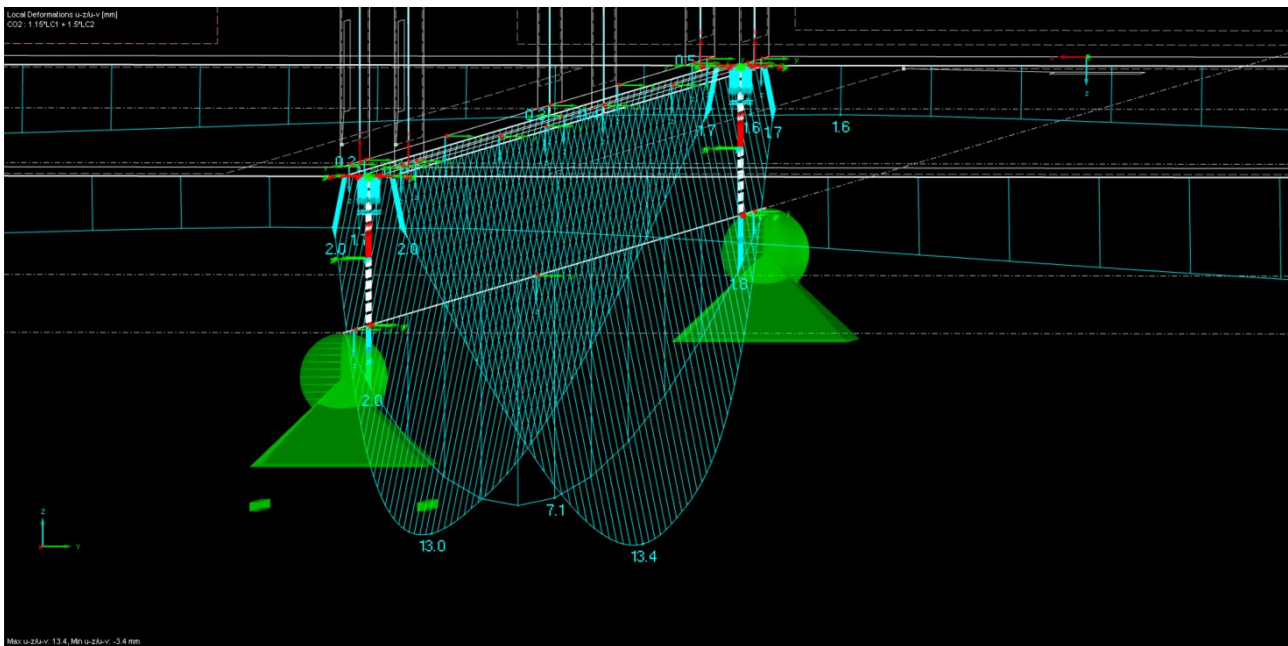
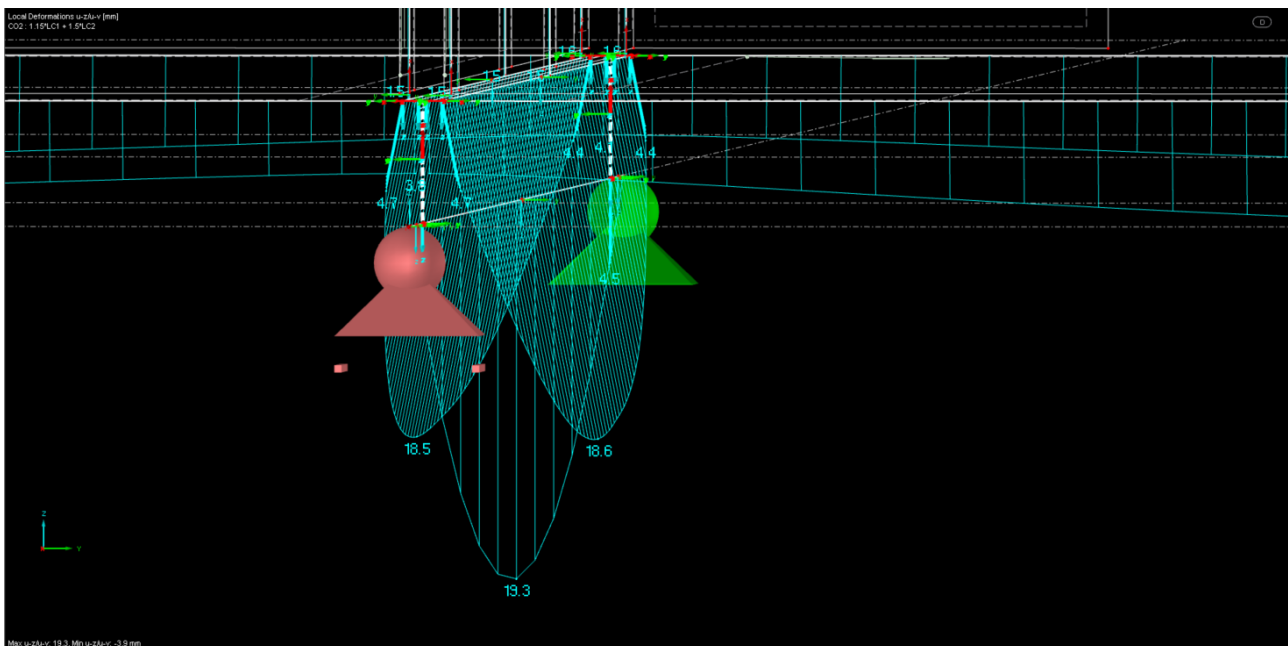


Figure 45. Local deflection of members in uz/uv with sliding hinges.



### 6.3.1 Results

All the models were found to be stable and behaving in a reasonable manner. The max global deflection in uz was found to be occurring in the same location in all three models, the middle concrete slab, and was found to be 13.5mm in the rigid hinge model, 14.1mm in the rotating hinge

model and 19.4 in the sliding hinge model. Focusing on local member deformation, similar results were found with max deflection occurring in the sliding hinge model where the largest openings in the LVL wall are located. In the rigid hinge model, the max deflection of the concrete was 12.7mm and the max deflection of the beams was 7.7mm. In the rotating hinge model, the max deflection of the concrete was 13.4mm and the max deflection of the beams was 7.1mm. In the sliding hinge model, the max deflection of the concrete was 18.6mm and the max deflection of the beams was 19.3mm.

The general conclusion based on these results was that all three hinge configurations are functional and behaving in a reasonable manner. However, the sliding configuration gave the largest deflections and was the only model where the deflection of the beam was larger than the concrete. Therefore, the sliding hinge configuration was determined to be the best choice and was used in the modelling of the structure for further analysis.

## **7 Simplified Analysis to Determine Size and Locations of the Sylomer Pads**

Due to the complexity of the model, it was decided to find the dimensions and locations of the sylomer pads by using simplified models. In this final phase of analysis, the focus was on the interaction of the materials and the geometry of the wall at one beam at a time.

### **7.1 Single Solid Wall, CFRHS200x200x12.5 beam**

First, a model was created with a solid LVL wall. Lateral stability was achieved by using supports preventing movement in the y-direction, connections between the floor and LVL were made with threaded bars, and all loads were applied as in the previous models. Next, to find the force occurring at the initial locations of the sylomer pads, the rigid bar series connecting the concrete floor to the main beam were changed to single RHS beams. The force was found to be 47.8 kN at both locations.

Figure 46. Simplified model of solid LVL wall with loads and supports visible.

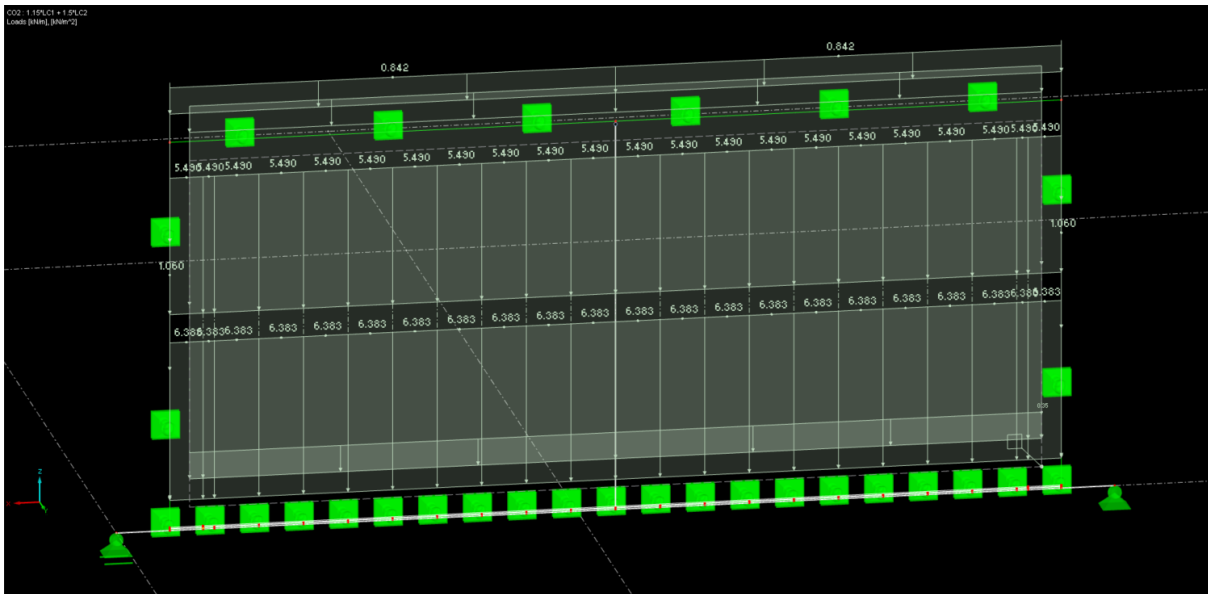
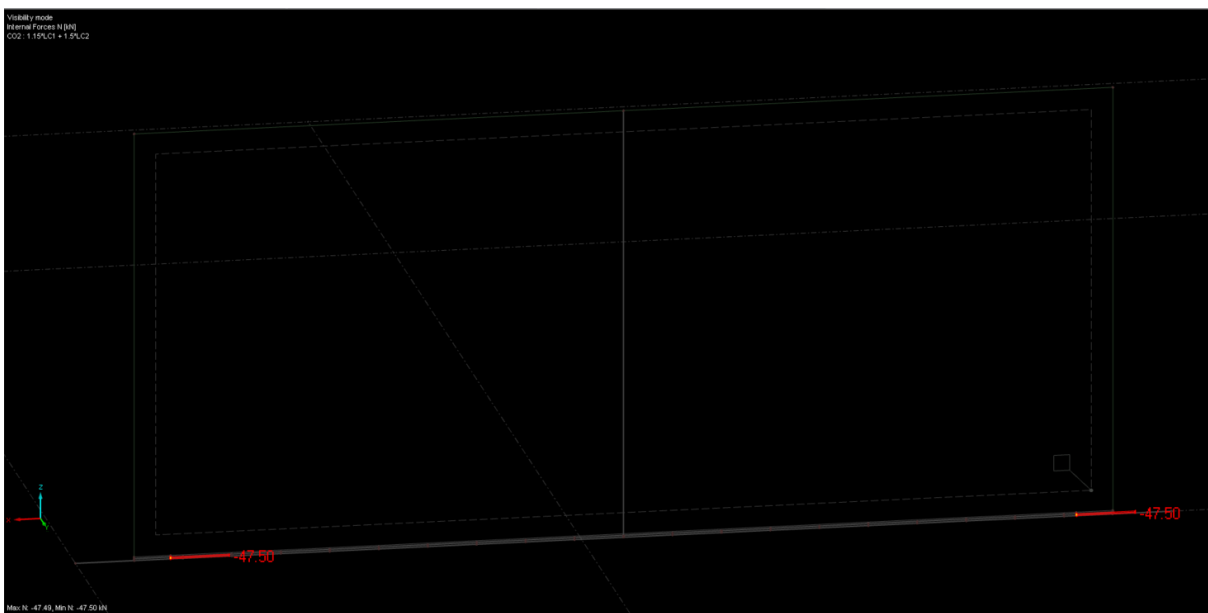
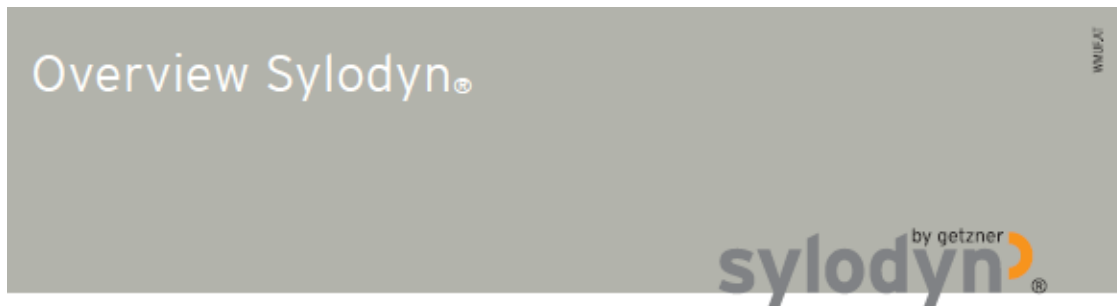


Figure 47. Force at the sylomer locations.



Next, the sylomer supplier was selected and material properties for the sylomer were found from the manufacturer's data sheet (see figure below). Sylodyn NF by Getzner was chosen to conduct the analysis. The applicable properties taken from the data sheet were the thickness (12.5mm), the static range of use (1.5 N/mm<sup>2</sup>) and the static modulus of elasticity (11.8 N/mm<sup>2</sup>) (Christian Berner Oy, 2019).

Figure 48. Product data sheet for Sylodyn by Getzner.

**Material**

closed-cell PU elastomer (polyurethane) with highly elastic properties

**Standard delivery dimension**

Thickness: 12.5 mm / 25 mm

Roll: 1.5 m wide, 5.0 m long

Strip: up to 1.5 m wide, up to 5.0 m long

Other dimensions, punched and moulded parts on request.

**Sylodyn<sup>®</sup> Material type**

**NB** **NC** **ND** **NE** **NF** **HRB HS 3000** **HRB HS 6000** **HRB HS 12000**

Material properties	Test methods	red	yellow	green	blue	violet	dark green	dark blue	dark brown
Colour		red	yellow	green	blue	violet	dark green	dark blue	dark brown
Static range of use <sup>1</sup> in N/mm <sup>2</sup>		0.075	0.150	0.350	0.750	1.500	3.000	6.000	12.000
Load peaks <sup>1</sup> in N/mm <sup>2</sup>		2.00	3.00	4.00	6.00	8.00	12.00	18.00	24.00
Mechanical loss factor	DIN 53513 <sup>2</sup>	0.07	0.07	0.08	0.09	0.10	0.07	0.07	0.08
Rebound resilience in %	EN ISO 8307	70	70	70	70	70	70	70	70
Compression set <sup>3</sup> in %	EN ISO 1856 <sup>2</sup>	<5	<5	<5	<5	<5	<5	<5	<5
Static modulus of elasticity <sup>1</sup> in N/mm <sup>2</sup>		0.75	1.10	2.55	6.55	11.80	33.20	74.00	181.00
Dynamic modulus of elasticity <sup>1</sup> in N/mm <sup>2</sup>	DIN 53513 <sup>2</sup>	0.90	1.45	3.35	7.70	15.20	49.10	113.80	323.00
Static shear modulus in N/mm <sup>2</sup>	DIN ISO 1827 <sup>2</sup>	0.13	0.21	0.35	0.61	0.80	2.40	3.50	4.00
Dynamic shear modulus in N/mm <sup>2</sup>	DIN ISO 1827 <sup>2</sup>	0.18	0.29	0.53	0.86	1.18	2.80	4.20	5.30
Min. tensile stress at rupture in N/mm <sup>2</sup>	DIN EN ISO 527-3/5/100 <sup>2</sup>	0.75	1.50	2.50	4.00	7.00	12.00	15.00	16.00
Min. tensile elongation at rupture in %	DIN EN ISO 527-3/5/100 <sup>2</sup>	450	500	500	500	500	400	400	400
Abrasion <sup>3</sup> in mm <sup>3</sup>	DIN EN ISO 4649	≤1,400	≤550	≤100	≤80	≤90	≤100	≤80	≤70
Coefficient of friction (steel)	Getzner Werkstoffe	0.7	0.7	0.7	0.7	0.7	0.7	0.7	0.4
Coefficient of friction (concrete)	Getzner Werkstoffe	0.7	0.7	0.7	0.7	0.7	0.7	0.7	0.6
Specific volume resistance in D·cm	DIN EN 62631-3-1 <sup>2</sup>	>10 <sup>6</sup>	>10 <sup>6</sup>	>10 <sup>6</sup>	>10 <sup>6</sup>	>10 <sup>6</sup>	>10 <sup>6</sup>	>10 <sup>6</sup>	>10 <sup>6</sup>
Thermal conductivity in W/mK	DIN EN 12667	0.060	0.075	0.090	0.100	0.110	0.160	0.170	0.190
Temperature range in °C		-30 to 70							
Temperature peak in °C	short term <sup>4</sup>	120							
Flammability	EN ISO 11925-2	class E/EN 13501-1							

<sup>1</sup> Values apply to shape factor q = 3

<sup>2</sup> Measurement/evaluation in accordance with the relevant standard

<sup>3</sup> The measurement is performed on a density-dependent basis with differing test parameters

<sup>4</sup> Application-specific

All information and data is based on our current knowledge. The data can be applied for calculations and as guidelines, are subject to typical manufacturing tolerances and are not guaranteed. Material properties as well as their tolerances can vary depending on type of application or use and are available from Getzner on request.

Further information can be found in VDI Guideline 2062 (Association of German Engineers) as well as in glossary. Further characteristic values on request.

Christian Berner Dy +358 9 2786 830 • info@christianberner.com • christianberner.fi

AUSTRIA – Bgls GERMANY – Berlin – Munich – Stuttgart FRANCE – Lyon JORDAN – Amman  
JAPAN – Tokyo INDIA – Pune CHINA – Beijing USA – Charlotte [www.getzner.com](http://www.getzner.com)

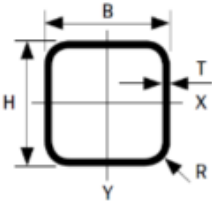
**getzner**  
engineering a quiet future

The dimensions of the Sylodyn NF pads were determined to be 125mm x 260mm with the calculations below. New members were then created in RFEM with the Sylodyn cross-section dimensions and material properties, and the model was recalculated.

Figure 49. Calculation of Sylodyn pad dimensions.

Determining max width of sylodyn pad according to the beam properties:

**TABLE 1**  
Dimension and cross sectional properties for SSAB Domex Tube, Strenx Tube 700 and SSAB Weathering Tube. Square hollow sections.



M = Weight  
 A = Cross-section area  
 A<sub>e</sub> = External surface area  
 I = Moment of inertia  
 W = Section modulus

W<sub>p</sub> = Plastic section modulus  
 i = Radius of gyration  
 I<sub>t</sub> = Torsion modulus  
 W<sub>t</sub> = Section modulus in torsion  
 Theoretical density = 7.85 kg/dm<sup>3</sup>

The cross-sectional properties have been calculated by using nominal dimensions H, B and T and corner outer radius R.

R = 2.0 x T, when T ≤ 6.0 mm  
 R = 2.5 x T, when 6.0 mm < T ≤ 10.0 mm  
 R = 3.0 x T, when T > 10.0 mm

Table 1 from the Structural Hollow Section properties publication by SSAB

$b_{steel} := 200 \text{ mm}$   
 $t_{steel} := 12.5 \text{ mm}$   
 $b_{Syl} := b_{steel} - 2 \cdot (3 \cdot t_{steel}) = 125 \text{ mm}$

Determining the length of the Sylodyn NF pad, single solid LVL wall:

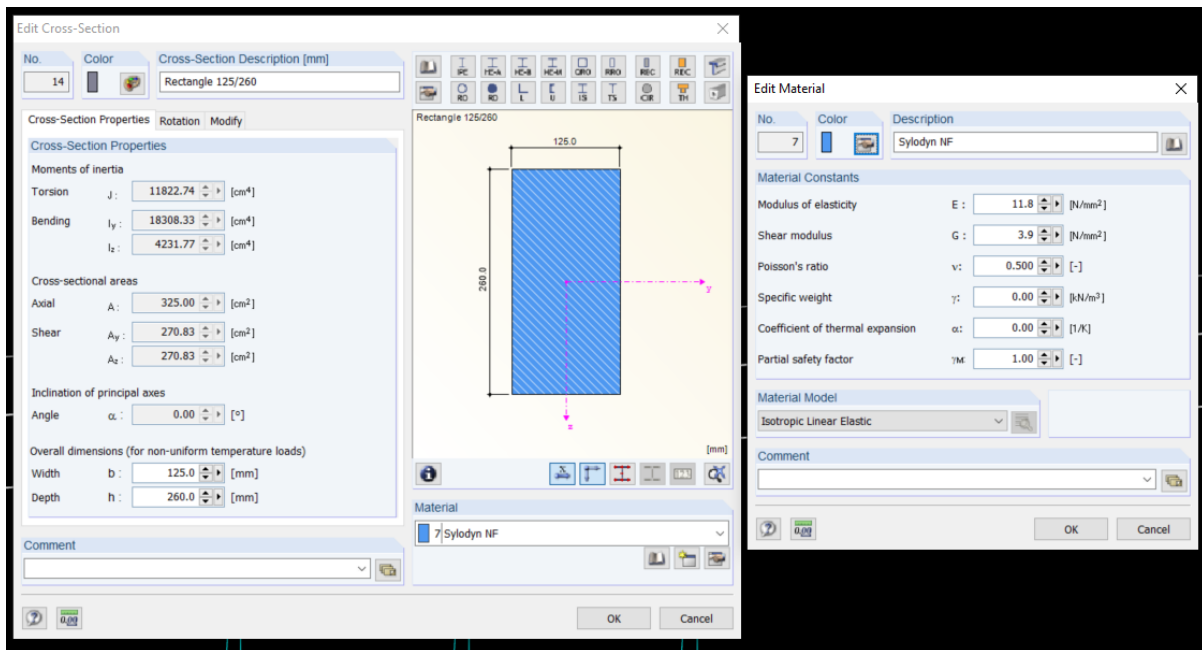
Using  $\sigma = \frac{F}{A}$  :

$\sigma_{SylNF} := 1.5 \frac{N}{mm^2}$

$F_{Single} := 48 \text{ kN}$  (RFEM)

$l_{Syl} := \frac{F_{Single}}{b_{Syl} \cdot \sigma_{SylNF}} = 256 \text{ mm} \rightarrow 260 \text{ mm}$

Figure 50. Cross-section and material properties of the Sylodyn.



### 7.1.1 Results

The model was successfully calculated, and the overall behaviour of the structure was reasonable. Focusing on the location of the sylomer on one side, the deflection of the concrete was found to be 7.2mm and the beam was 5.8mm. This means that the Sylodyn pad is compressing 1.4mm. After making a hand calculation, this was verified (see calculations below). Next, a check was made between the first Sylodyn pad and the centre of the structure to verify that there was no clashing between the concrete and beam. The maximum deflection of the concrete was found to be 22.1mm, and the beam in the same location was 13.3mm. Taking the original 12.5mm gap between the concrete and beam into account, there was a 3.7mm gap after loading, verifying that there was no clashing. Therefore, the results show that two 125mmx260mm Sylodyn NF pads located on the ends of the module directly below the LVL-concrete threaded bar connection are sufficient for supporting a single solid wall module on a CFRHS200x200x12.5 beam.

Figure 51. Deflection of the concrete and beam.

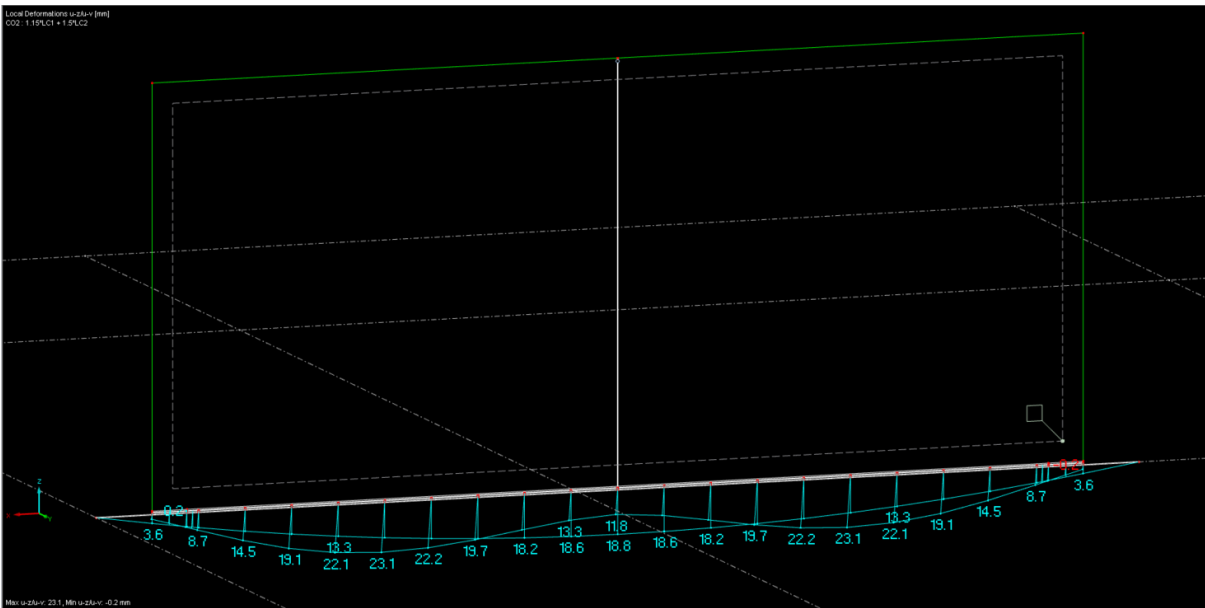


Figure 52. Deflection of the concrete and beam at the Syldodyn pad.

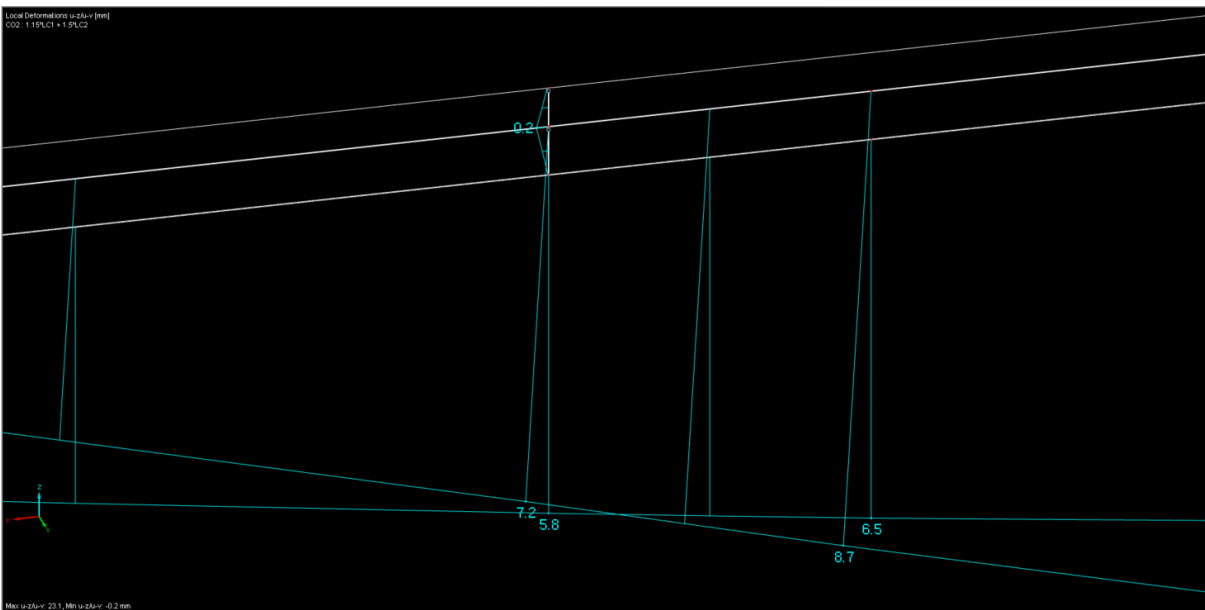




Figure 53. Verification of compression in the Sylodyn pad.

**VERIFICATION OF COMPRESSION IN SYLODYN PAD**

$$F_{Syl} := 48 \text{ kN}$$

$$L_{Syl} := 12.5 \text{ mm}$$

$$A_{Syl} := b_{Syl} \cdot l_{Syl}$$

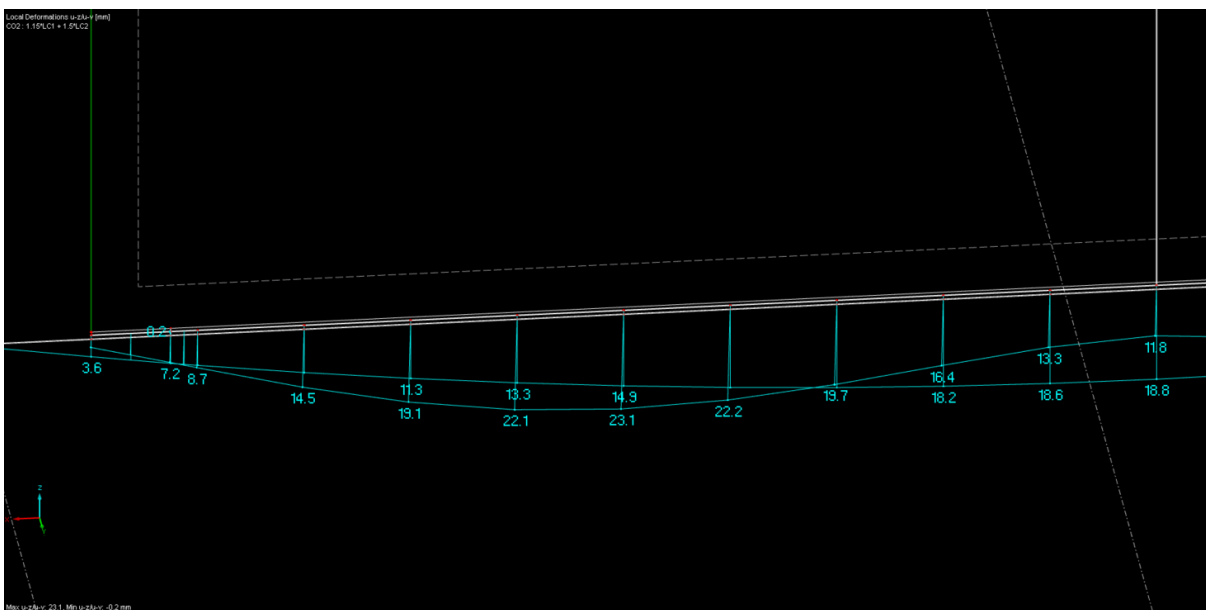
$$E_{Syl} := 11.8 \frac{\text{N}}{\text{mm}^2}$$

$$\delta_{Syl} := \frac{(F_{Syl} \cdot L_{Syl})}{A_{Syl} \cdot E_{Syl}} = 1.589 \text{ mm}$$

$$\delta_{SylModel} := 7.2 \text{ mm} - 5.8 \text{ mm} = 1.4 \text{ mm}$$

**OKAY!!!**

Figure 54



Deflection of the concrete and beam between the first Sylodyn pad and the centre of the wall.

## 7.2 Double Solid Wall, CFRHS200x200x12.5 beam

After the design scenario above involving a single wall was verified, the results of a loading from two LVL walls was checked. Since the deflection of each LVL wall from the concrete load would be the same as already calculated, and because the deflection of the steel beam is the important factor in this phase of analysis, it was decided to reduce the beam profile to CFRHS200x200x6. Reducing the profile thickness additionally provided a larger factor of safety to the results, due to the profile thickness of 6 mm being more than half of the original thickness of 12.5 mm. The forces at the sylomer locations were verified to be the same as in the previous model, so the same Sylodyn pad dimensions were used. However, the forces from two walls will be twice as high, so with these dimensions, the Sylodyn grade will have to be increased to HRB HS 3000, which has a static range of use of  $3.0 \text{ N/mm}^2$ . If Sylodyn NF is used, the length of each pad should be doubled (see calculations below).

Figure 55. Force at the sylomer locations.

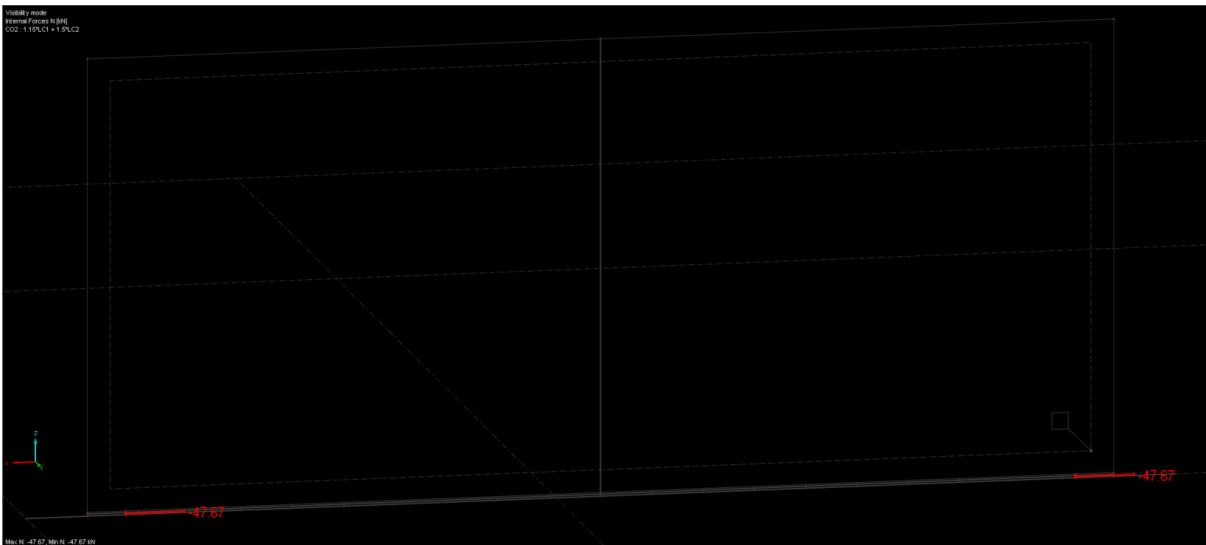


Figure 56. Calculations determining the length of Sylodyn HRB HS 3000 and Sylodyn NF for a double solid wall.

Determining the length of the Sylodyn HRB HS 3000 pad, Double solid LVL wall:

Using  $\sigma = \frac{F}{A}$  :

$$\sigma_{SylHRB} := 3 \frac{N}{mm^2}$$

$$F_{Double} := 2 \cdot 48 \text{ kN} \quad (\text{RFEM})$$

$$l_{Syl} := \frac{F_{Double}}{b_{Syl} \cdot \sigma_{SylHRB}} = 256 \text{ mm} \rightarrow 260 \text{ mm}$$

Determining the length of the Sylodyn NF pad, Double solid LVL wall:

Using  $\sigma = \frac{F}{A}$  :

$$\sigma_{SylNF} := 1.5 \frac{N}{mm^2}$$

$$F_{Double} := 2 \cdot 48 \text{ kN} \quad (\text{RFEM})$$

$$l_{Syl} := \frac{F_{Double}}{b_{Syl} \cdot \sigma_{SylNF}} = 512 \text{ mm} \rightarrow 520 \text{ mm}$$

### 7.2.1 Results

The model was successfully calculated, and the overall behaviour of the structure was reasonable. The deflection of the beam was larger than in the previous model, as expected. The maximum deflection of the concrete between the first Sylodyn pad and the centre of the structure was found to be 22.7mm, and the beam in the same location was 18.3mm. Taking the original 12.5mm gap between the concrete and beam into account, there was an 8.1mm gap after loading, verifying that there was no clashing. The max beam deflection of 30.3mm exceeds the SLS deflection limit of 23mm (see beam calculations), so pre-cambering of the beam will be required. With this pre-cambering, the results show that two 125mmx260mm Sylodyn HRB HS 3000 pads (or two 125mmx520mm Sylodyn NF pads) located on the ends of the module directly below the LVL-

concrete threaded bar connection are sufficient for supporting a double solid wall module on a CFRHS200x200x12.5 beam.

Figure 57. Deflection of the concrete and beam.

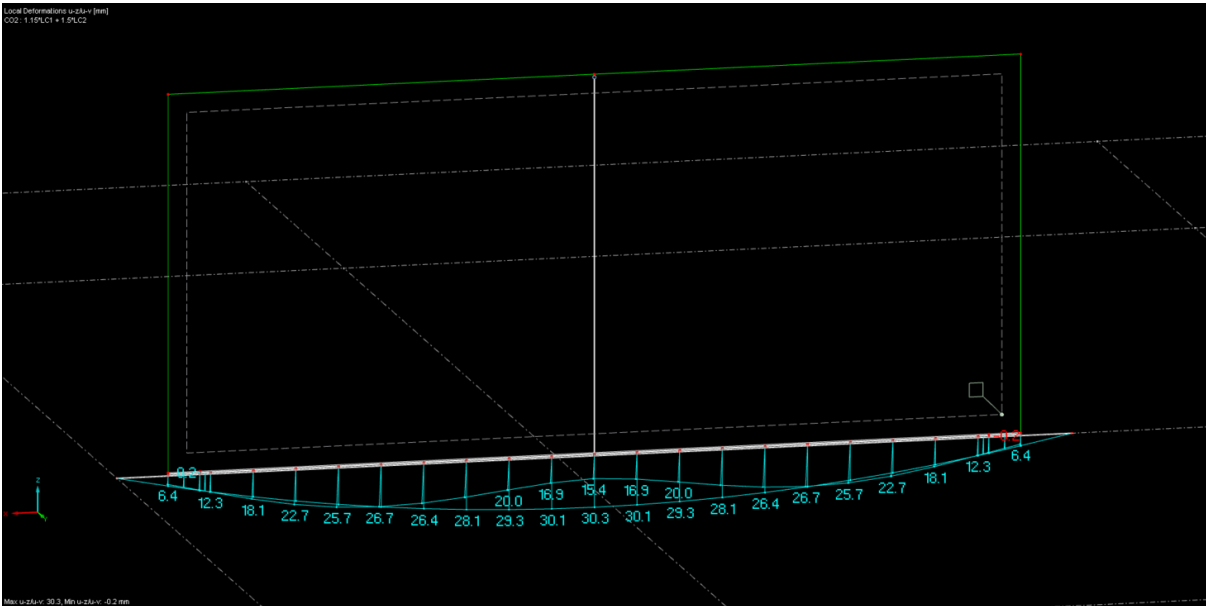
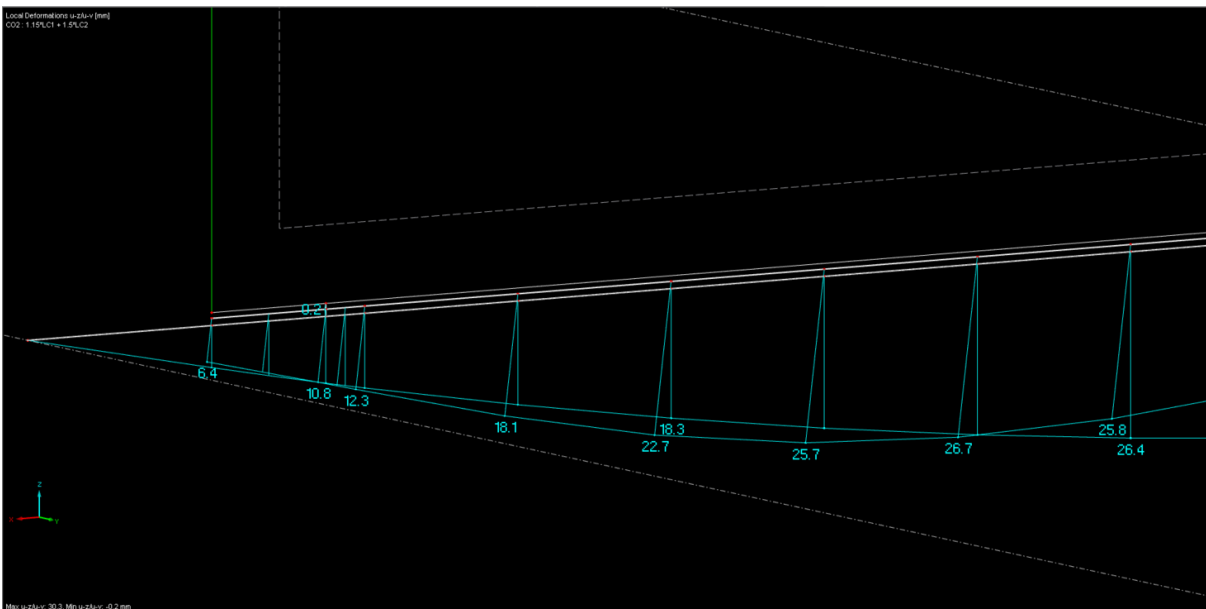


Figure 58. Deflection of the concrete and beam between the first Syldodyn pad and the centre of the wall.



### 7.3 Single wall with opening, CFRHS200x200x12.5 beam

The same analysis applied to the solid wall was next applied to a wall with an opening. First, the model was calculated with the sylomer pads located beneath the threaded bars at the ends. In this scenario, the concrete was found to be deflecting 46.0mm at the same location where the beam was deflecting 15.3mm, showing that clashing was occurring. Another sylomer pad was then added at this location on the beam and, after recalculating the model, it was found that the clashing was prevented. From this model, the forces at the sylomer locations were found, the Sylodyn pad dimensions were determined (see calculations below), and the pad properties were input into the model.

Figure 59. Deflection of the concrete and beam with two sylomer pads.

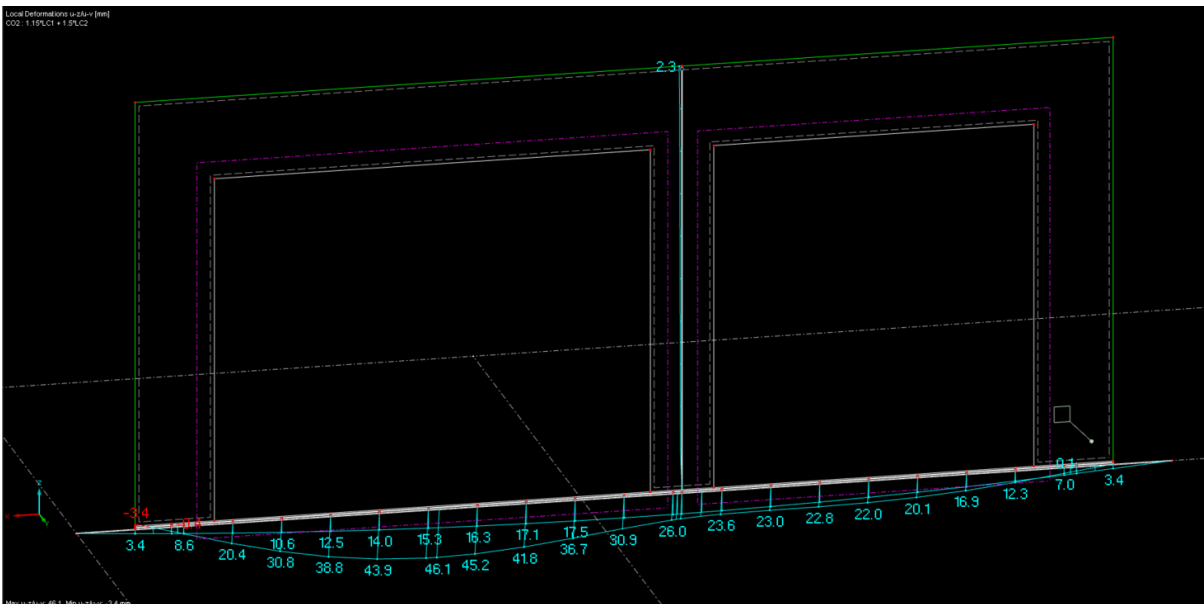


Figure 60. Deflection of the concrete showing clashing with the beam.

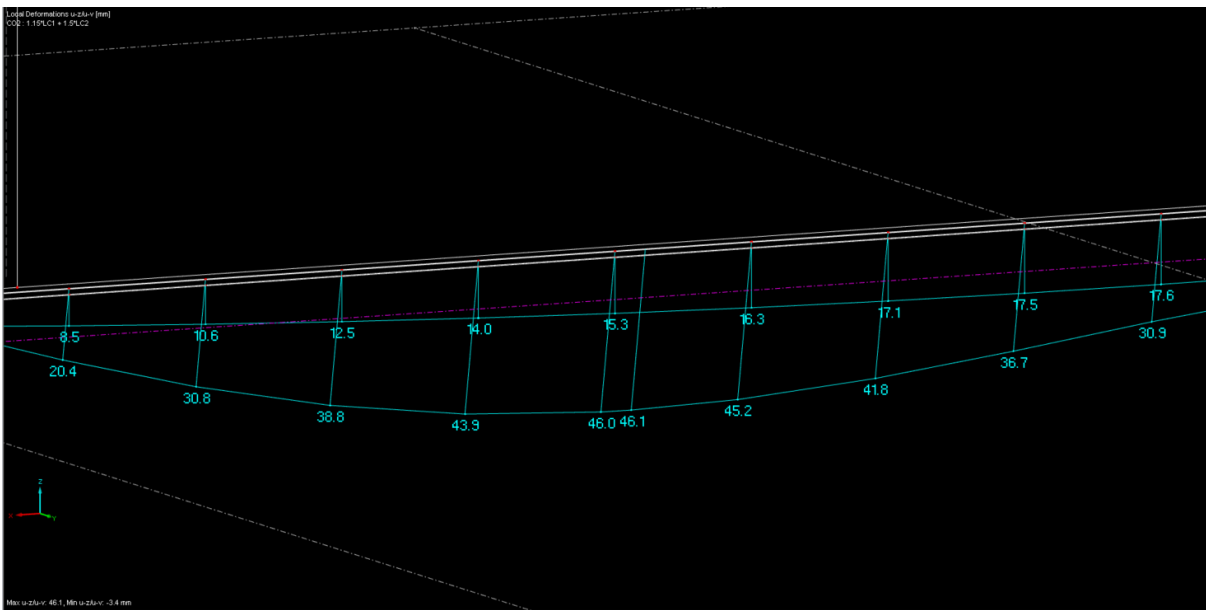


Figure 61. Deflection of the concrete and beam with three sylomer pads, clashing was prevented.

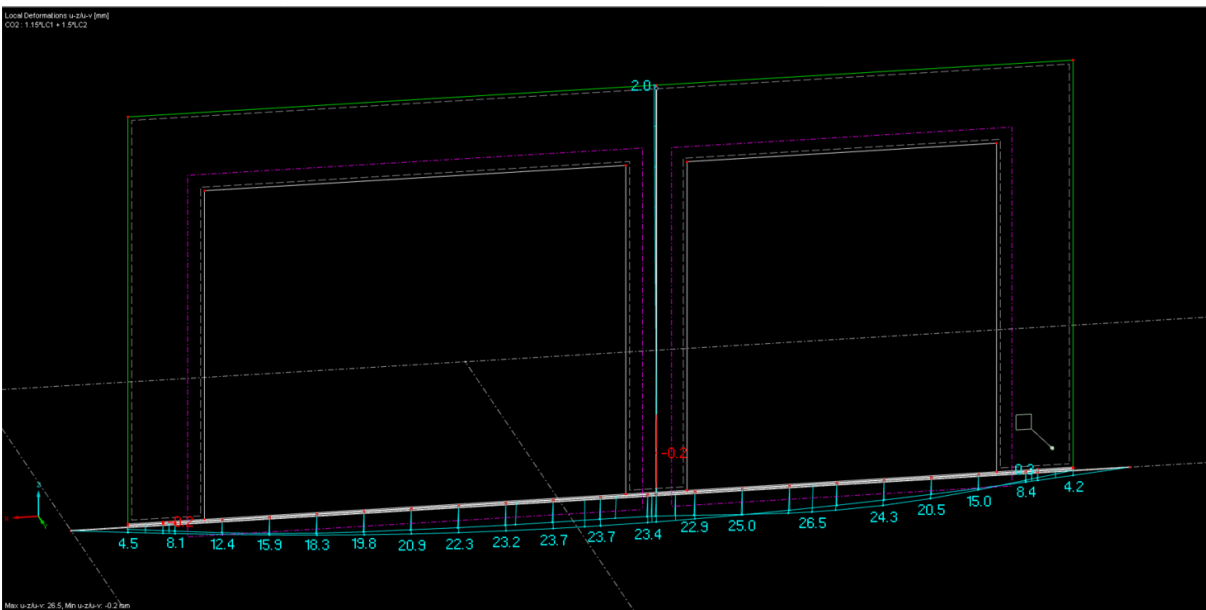


Figure 62. Force at the sylomer locations.

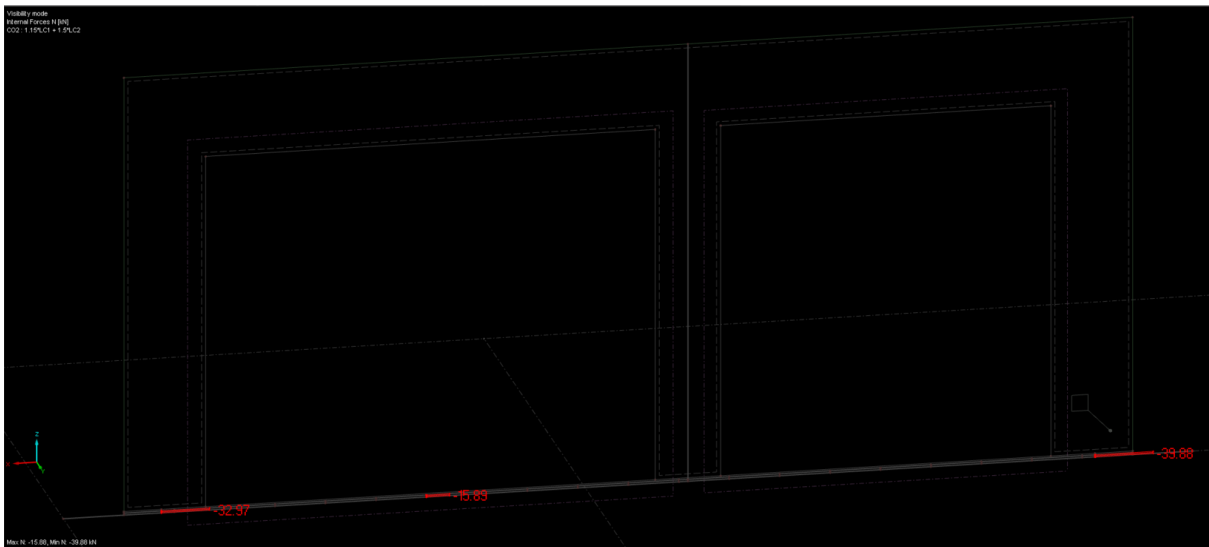


Figure 63. Calculations determining the length of Sylodyn NF for a single LVL wall with opening.

Determining the length of the sylodyn pad, opening LVL wall 1:

$$b_{Syl} := b_{steel} - 2 \cdot (3 \cdot t_{steel}) = 125 \text{ mm}$$

Using  $\sigma = \frac{F}{A}$  :

Location a:

$$F_{Syl\_a} := 33 \text{ kN(RFEM)}$$

$$\sigma_{Syl} := 1.5 \frac{N}{mm^2}$$

$$l_{Syl\_a} := \frac{F_{Syl\_a}}{b_{Syl} \cdot \sigma_{Syl}} = 176 \text{ mm} \quad \rightarrow 180 \text{ mm}$$

Location b:

$$F_{Syl\_b} := 16 \text{ kN(RFEM)}$$

$$\sigma_{Syl} := 1.5 \frac{N}{mm^2}$$

$$l_{Syl\_b} := \frac{F_{Syl\_b}}{b_{Syl} \cdot \sigma_{Syl}} = 85.333 \text{ mm} \quad \rightarrow 90 \text{ mm}$$

Location c:

$$F_{Syl\_c} := 40 \text{ kN(RFEM)}$$

$$\sigma_{Syl} := 1.5 \frac{N}{mm^2}$$

$$l_{Syl\_c} := \frac{F_{Syl\_c}}{b_{Syl} \cdot \sigma_{Syl}} = 213.333 \text{ mm} \quad \rightarrow 215 \text{ mm}$$

### 7.3.1 Results

The updated model was calculated, and the overall behaviour of the structure was reasonable.

The deflection of the concrete was found to be 24.4mm where the beam in the same location was 16.0mm. Taking the original 12.5mm gap between the concrete and beam into account, there was an 4.1mm gap after loading, verifying that there was no clashing. The max beam deflection of



23.8mm exceeds the SLS deflection limit of 23mm (see beam calculations), so pre-cambering of the beam will be required. With this pre-cambering, the results show that three Syldyn pads will be required to support a single module wall with this geometry on a CFRHS200x200x6 beam. The locations of the pads are dimensioned below, with the size of the first pad from the left being 125mmx180mm, the second being 125mmx90mm and the third being 125mmx215mm.

Figure 64. Deflection of the concrete and beam where clashing check was made.

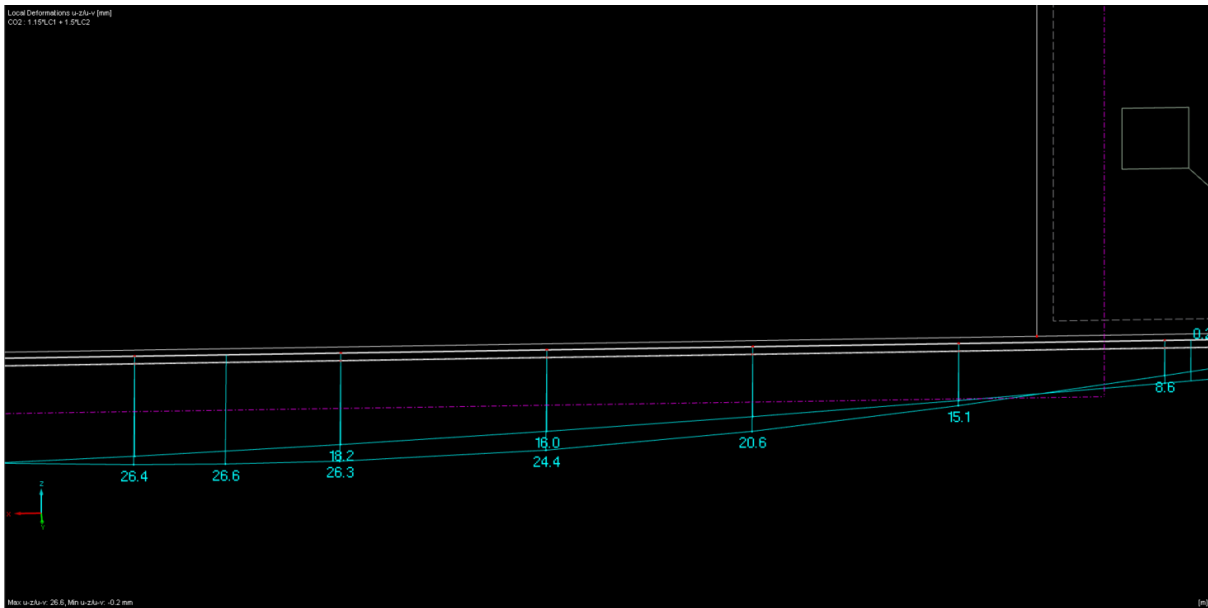
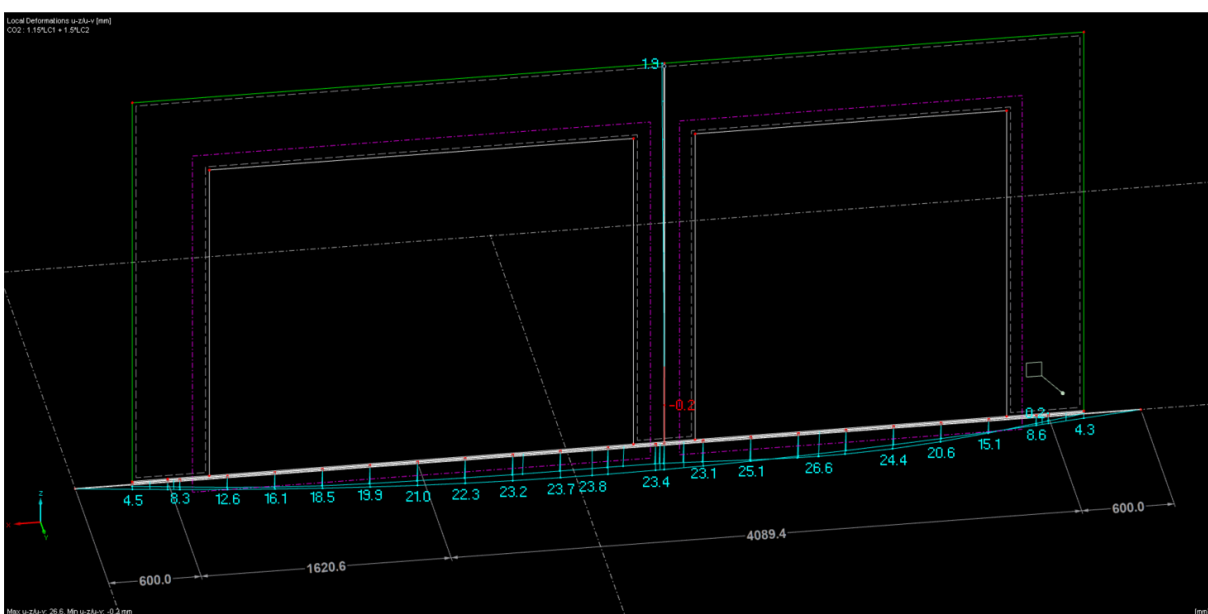


Figure 65. Results with three pad locations dimensioned.



## 7.4 Double wall with opening, CFRHS200x200x12.5 beam

As with the solid wall analysis, a loading from two LVL walls was analysed by decreasing the beam profile to CFRHS200x200x6. Like the previous opening wall analysis, two sylomer locations were used to start with. After calculating the model, the concrete was found to be deflecting 49.5mm at the same location where the beam was deflecting 24.6mm, showing that clashing was occurring. Another sylomer pad was then added at this location on the beam and, after recalculating the model, it was found that the clashing was prevented. From this model, the forces at the sylomer locations were found and the pads were dimensioned accordingly. However, the forces from two walls will be twice as high, so with these dimensions, the Sylodyn grade will have to be increased to HRB HS 3000, which has a static range of use of  $3.0 \text{ N/mm}^2$ . If Sylodyn NF is used, the length of each pad should be doubled (see calculations below).

Figure 66. Deflection of the concrete and beam with two sylomer pads.

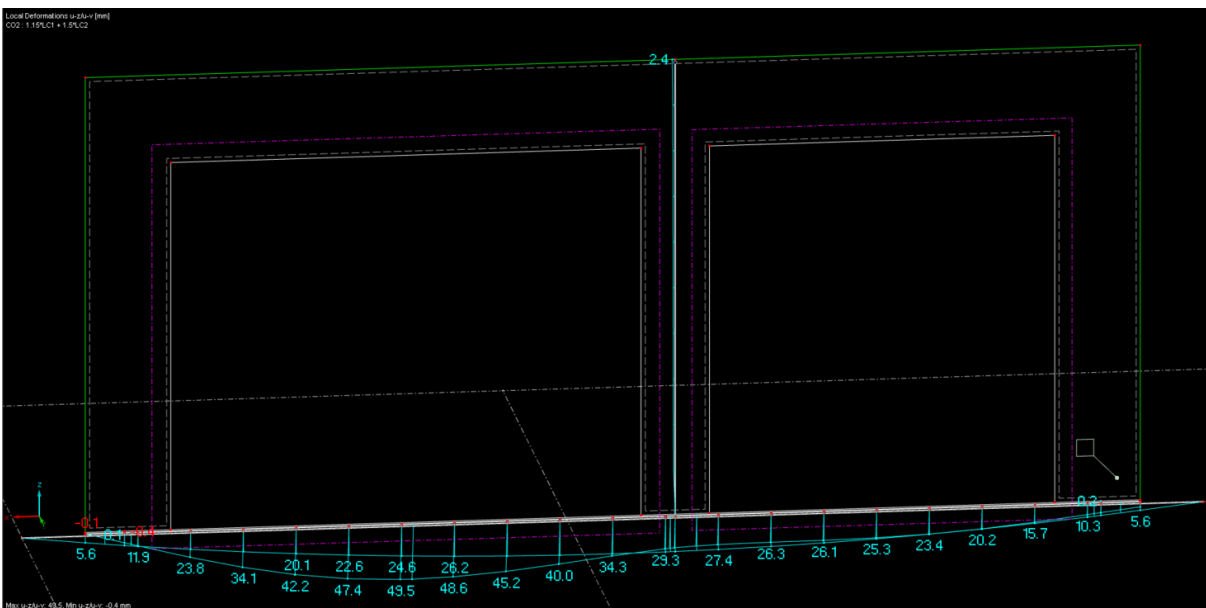


Figure 67. Deflection of the concrete showing clashing with the beam.

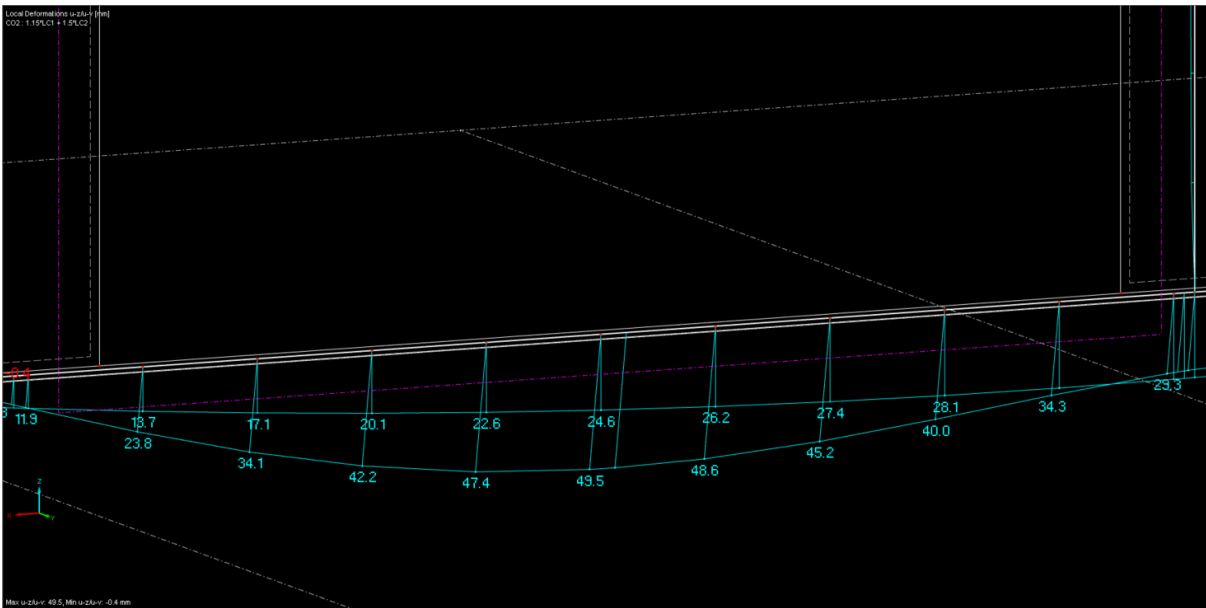


Figure 68. Force at the sylomer locations.

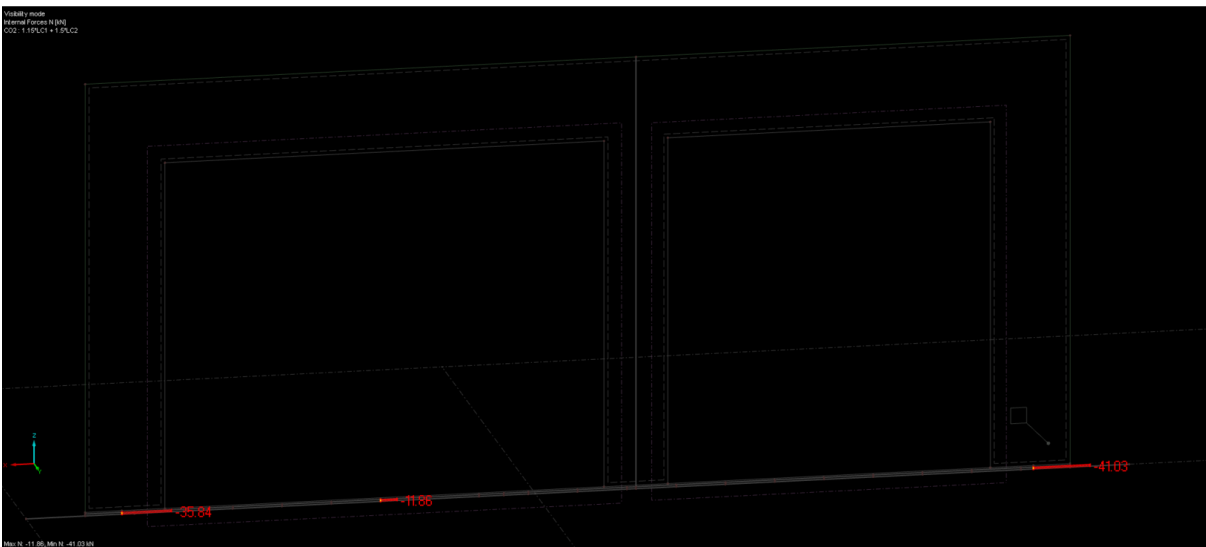


Figure 69. Calculations determining the length of Sylodyn HRB HS 3000 for a double LVL wall with opening.

Determining the length of the Sylodyn HRB HS 3000 pad, Double wall with opening:

$$b_{Syl} := b_{steel} - 2 \cdot (3 \cdot t_{steel}) = 125 \text{ mm}$$

Using:  $\sigma = \frac{F}{A}$

$$\sigma_{SylHRB} := 3 \frac{N}{mm^2}$$

Location a:

$$F_{Double\_a} := 2 \cdot 36 \text{ kN} \quad (\text{RFEM})$$

$$l_{Syl\_a} := \frac{F_{Double\_a}}{b_{Syl} \cdot \sigma_{SylHRB}} = 192 \text{ mm} \quad \rightarrow 195 \text{ mm}$$

Location b:

$$F_{Double\_b} := 2 \cdot 12 \text{ kN} \quad (\text{RFEM})$$

$$l_{Syl\_b} := \frac{F_{Double\_b}}{b_{Syl} \cdot \sigma_{SylHRB}} = 64 \text{ mm} \quad \rightarrow 65 \text{ mm}$$

Location c:

$$F_{Double\_c} := 2 \cdot 42 \text{ kN} \quad (\text{RFEM})$$

$$l_{Syl\_c} := \frac{F_{Double\_c}}{b_{Syl} \cdot \sigma_{SylHRB}} = 224 \text{ mm} \quad \rightarrow 225 \text{ mm}$$

Figure 70. Calculations determining the length of Sylodyn NF for a double LVL wall with opening.

Determining the length of the Sylodyn NF pad, Double wall with opening:

$$b_{Syl} := b_{steel} - 2 \cdot (3 \cdot t_{steel}) = 125 \text{ mm}$$

Using  $\sigma = \frac{F}{A}$  :

$$\sigma_{SylNF} := 1.5 \cdot \frac{N}{\text{mm}^2}$$

Location a:

$$F_{Double\_a} := 2 \cdot 36 \text{ kN} \quad (\text{RFEM})$$

$$l_{Syl\_a} := \frac{F_{Double\_a}}{b_{Syl} \cdot \sigma_{SylNF}} = 384 \text{ mm} \quad \rightarrow 390 \text{ mm}$$

Location b:

$$F_{Double\_b} := 2 \cdot 12 \text{ kN} \quad (\text{RFEM})$$

$$l_{Syl\_b} := \frac{F_{Double\_b}}{b_{Syl} \cdot \sigma_{SylNF}} = 128 \text{ mm} \quad \rightarrow 130 \text{ mm}$$

Location c:

$$F_{Double\_c} := 2 \cdot 42 \text{ kN} \quad (\text{RFEM})$$

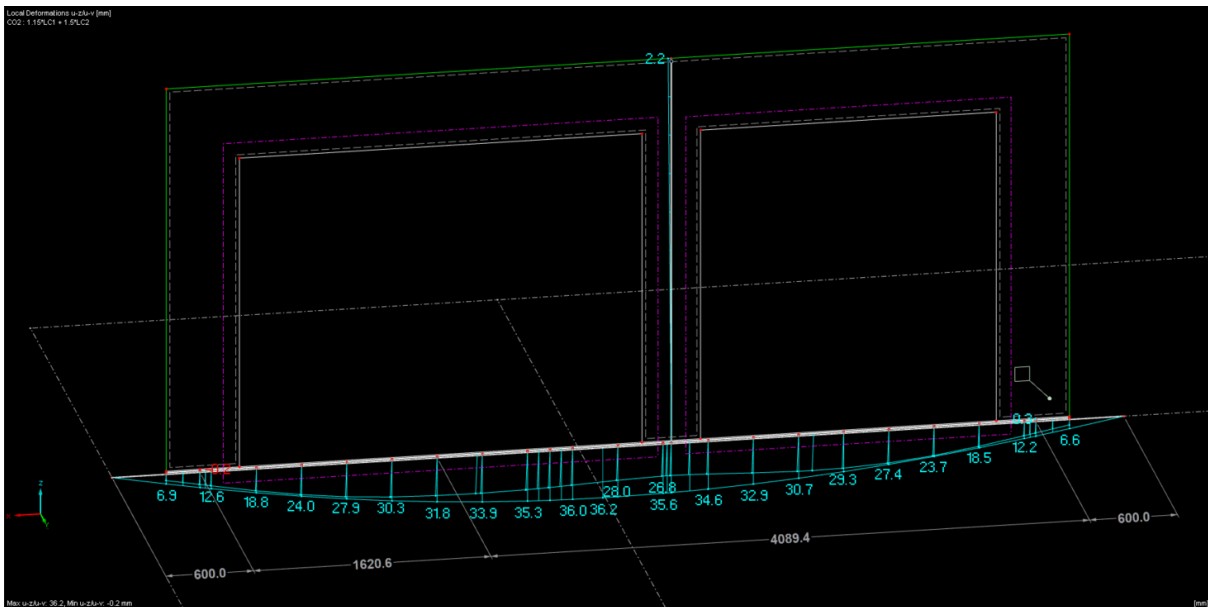
$$l_{Syl\_c} := \frac{F_{Double\_c}}{b_{Syl} \cdot \sigma_{SylNF}} = 448 \text{ mm} \quad \rightarrow 450 \text{ mm}$$

#### 7.4.1 Results

The updated model was calculated, and the overall behaviour of the structure was reasonable. The deflection of the concrete was found to be less than the beam throughout the entire span, verifying that there was no clashing. The max beam deflection of 36.2mm exceeds the SLS deflection limit of 23mm (see beam calculations), so pre-cambering of the beam will be required. With this pre-cambering, the results show that three Sylodyn pads will be required to support two

module walls with this geometry on a CFRHS200x200x12 beam, with the pad locations dimensioned in the image below. See above calculations for pad grade and sizes.

Figure 71. Results with three pad locations dimensioned.



## 8 Conclusion

Through the analysis conducted in this thesis, results were obtained for all key research questions, as follows below.

- What material primarily carries the loads in the units?

The material in the unit which primarily carries the loads was found to be the LVL when the wall is solid (see section 6.2). In cases where there are openings in the walls, loads from the concrete floor may also need to be supported by the steel beam via a Syldon sylomer pad (see sections 7.3 and 7.4).

- What is the best way to model the design situation?

The best way to model the design situation is to treat the LVL as a surface in the RFEM model (see section 6.2). A simplified model which focuses on the unique geometry and loading occurring at each beam is the most useful way to analyze the interface between the

timber-concrete units and the steel beam in order to determine the need and location of added support from the sylomer pads (see section 7). The sylomer pads should be modeled using a pinned-sliding hinge configuration (see section 6.3).

- How do the timber-concrete units interact with the steel frame?

It was found that the timber-concrete units and steel frame act as a composite structure in two ways. First, when the LVL wall is solid, the loading from the concrete floor is fully supported by the LVL, and the loading from the unit is supported at two points by the steel beam (see sections 7.1 and 7.2). Second, when the LVL wall has openings, the loading from the concrete floor is partly supported by the LVL, and partly supported by additional contact points on the steel beam (see sections 7.3 and 7.4).

- What contact points are needed between the frame and units?

The needed contact points between the frame and the units were dependent on the geometry of the LVL wall and the number of walls on the beam (see section 7). The required contact points in the cases analyzed in this thesis are summarized in the following table.

Table 1. Summary of results for needed contact points.

	<b># of contact points</b>	<b>Dimensions (Sylodyn NF)</b>	<b>Dimensions (Sylodyn HRB HS 3000)</b>
<b>Single Solid Wall (see section 7.1)</b>	2	<b>Location a, b:</b> 125x260x12.5 (600 mm from ends of beam)	N/A
<b>Double Solid Wall (see section 7.2)</b>	2	<b>Location a, b:</b> 125x520x12.5 (600 mm from ends of beam)	<b>Location a, b:</b> 125x260x12.5 (600 mm from ends of beam)
<b>Single opening (see section 7.3)</b>	3	<b>Location a:</b> 125x180x12.5 <b>Location b:</b> 125x90x12.5 <b>Location c:</b> 125x215x12.5 (see Fig. 64 for locations)	N/A
<b>Double opening wall (see section 7.4)</b>	3	<b>Location a:</b> 125x390x12.5 <b>Location b:</b> 125x130x12.5 <b>Location c:</b> 125x450x12.5 (see Fig. 70 for locations)	<b>Location a:</b> 125x195x12.5 <b>Location b:</b> 125x65x12.5 <b>Location c:</b> 125x225x12.5 (see Fig. 70 for locations)

In addition to finding results for the key research questions above, it was also found that the profile thickness of the steel beams needs to be increased to 12.5mm and precambering will be required (see section 3.2), and that the smallest allowable height of the LVL in case of a full-span opening is 840mm (see section 3.3).



While results were obtained for all key research questions in this thesis, it is important to note that these results are only preliminary. An analysis must be conducted for each different opening scenario in order to find sylomer locations and dimensions, and more detailed verifications of the capacities of the beams, connections, and the stability of the structure still need to be carried out. Nevertheless, the models developed in this thesis can be used to continue analysis and design of this particular building, and they can also be used in the future as a starting point for analyzing similar structures utilizing the same building system.

## References

Christian Berner Oy. (2019). *Product data sheet, Sylodyn by Getzer*. Retrieved from

<https://www.christianberner.fi/globalassets/leverantorer/getzner-werkstoffe-gmbh/dokument/finland/data-sheet-overview-sylodyn-en.pdf>

Finnish Ministry of the Environment. (2019). *National Building Code of Finland: Strength and*

*Stability of Structures: Steel Structures*. Retrieved from <https://ym.fi/en/the-national-building-code-of-finland>

PUUINFO. (2020). *Puurakenteiden Lyhennetty Suunnitteluohje*. Retrieved from

<https://puuinfo.fi/suunnittelu/ohjeet/eurokoodi-5-lyhennetty-suunnitteluohje/>

Structx. (2021). *Beam Design Formulas: Continuous Beams – Two Equal Spans with UDL*.

Retrieved from [https://structx.com/Beam\\_Formulas\\_041.html](https://structx.com/Beam_Formulas_041.html)

Structx. (2021). *Beam Design Formulas: Simple Beam – Point load at center*. Retrieved from

[https://structx.com/Beam\\_Formulas\\_007.html](https://structx.com/Beam_Formulas_007.html)